

Project Acronym	CORMORAN (ANR 11-INFR-010)
Document Title	D4.1 - Demonstration Scenarios and Interfaces between Algorithms and Platforms
Contractual Date of Delivery	M30 (31/06/2014) - M33 (30/09/2014) [Approved Extension]
Actual Date of Delivery	M33
Editors	Benoît Denis (CEA)
Authors	Benoît Denis, Lionel Biard (CEA), Claire Goursaud, Arturo Guizar (INSA), Jihad Hamie, Claude Chaudet (TPT), Bernard Uguen, Nicolas Amiot, Stéphane Avrillon, Meriem Mhedhbi (UR1)
Participants	CEA, INSA, TPT, UR1
Related Task(s)	T4
Related Sub-Task(s)	ST4.1 & ST4.2
Security	Public
Nature	Technical Report
Version Number	1.0
Total Number of Pages	65

Key words: demonstration scenarios, field experiments, integrated radio devices, measurement database, motion capture, personal navigation, wireless on-body nodes.

Contacts & Correspondence

Benoît Denis (CEA)

- Address: CEA-Leti Minatec, 17 rue des Martyrs, Bât. 51C, p. C455, 38054 GRENOBLE Cedex 9, France
- E-mail: benoit.denis@cea.fr
- Tel: + 33 (0)4 38 78 09 90

TABLE OF CONTENT

TABLE OF CONTENT	3
TABLE OF ACRONYMS	4
ABSTRACT	5
1. INTRODUCTION.....	6
2. INVOLVED RADIO DEVICES AND REFERENCE OPTICAL SYSTEMS.....	7
2.1. Radio Devices	7
2.1.1 CEA’s IR-UWB TCR Devices	7
2.1.2 BeSpoon’s IR-UWB SpoonPhone and Tag Devices	9
2.1.3 HikoB’s IEEE 802.15.4 FOX Devices	10
2.2. Optical Capture Systems & Video Means	11
2.2.1 CodaMotion	11
2.2.2 Vicon	12
3. EXPERIMENTAL SET-UP AND SCENARIOS	13
3.1. First Measurement/Demonstration Campaign.....	13
3.1.1 Test Environment	14
3.1.2 Scenarios	14
3.2. Second Measurement/Demonstration Campaign.....	19
3.2.1 Test Environment	19
3.2.2 Scenarios	20
4. FIRST POST-PROCESSING STEPS AND RESULTING MEASUREMENT/DEMONSTRATION DATABASE	29
4.1. Post-Synchronization of Radio and MoCap Traces	29
4.2. Demonstration/Measurement Database Access and Exploitation	32
4.2.1 Exploitation in the PyLayers Framework	33
4.2.2 Exploitation as Matlab Files	54
5. CONCLUSION	57
APPENDICES	58
5.1. Appendix 1: Measurement Log and Meta Data (2 nd Campaign).....	58
5.1.1 Day 1: Motion Capture and Mobility Detection Scenarios	58
5.1.1 Day 2: Navigation Scenarios	61
REFERENCES	64

TABLE OF ACRONYMS

AP	Access Point (WLAN)
CAP	Contention Access Phase
CDWMDS	Constrained Distributed Weighted Multi-Dimensional Scaling
CFP	Contention Free Period
CGN	Coordinated Group Navigation
CSMA/CA	Carrier Sense Multiple Access with Collision Avoidance
D(B)PSK	Differential (Binary) Phase Shift Keying
FAP	First Arrival Path
GTS	Guaranteed Time Slots
IR-UWB	Impulse Radio – Ultra Wideband
ISM	Industrial Scientific & Medical radio bands
LCS	Local Coordinates System
LDR-LT	Low Data Rate – Location and Tracking
MAC	Medium Access Control layer
LoS	Line of Sight
LSIMC	Large-Scale Individual Motion Capture
MoCap	Motion Capture
NB	Narrow Band
NLoS	Non-Line of Sight
NWK	NetWorK layer
PHY	PHYSical layer
QoS	Quality of Service
RSSI	Received Signal Strength Indicator
(RT-)ToF	(Round Trip -) Time Of Flight
Rx	Receiver
SNR	Signal to Noise Ratio
TDMA	Time Division Multiple Access
ToA	Time of Arrival
TWR	Two Way Ranging
Tx	Transmitter
WBAN	Wireless Body Area Network
WLAN	Wireless Local Area Network
WPAN	Wireless Personal Area Network
WSN	Wireless Sensor Network

ABSTRACT

Wireless Body Area Networks, which currently benefit from the emergence of *Ultra Low Power* radio technologies, like the *Impulse Radio - Ultra Wideband*, may be massively disseminated in the public space in the near future, as distributed elements of a more global heterogeneous communication architecture. Besides, user-centric and context-aware services have been progressing significantly for the last past years, requiring e.g. that the location information is delivered on the mobile user side, with a limited access to the infrastructure. In the context of wearable networks, new cooperative communication schemes, involving peer-to-peer radio links between mobile nodes or terminals, provide natural interactions at the body scale (i.e. on-body cooperation) and/or between mobile users (i.e. body-to-body cooperation). The cooperative links are thus not only expected to improve data rates, communication robustness or coverage, but they shall also enable to retrieve relative range measurements, based on transmitted signals (e.g. based on *Round Trip - Time of Flight* or *Received Signal Strength*). The CORMORAN project aims at investigating such cooperation mechanisms *in* and *between* body area networks, mostly for large scale individual motion capture and coordinated group navigation applications. Determining the adequate cooperation level and modes will help to achieve a precise radiolocation of on-body nodes and/or pedestrians, as well as an optimal management of the communication quality of service at the protocol level. One more stake consists in taking into account the highly specific characteristics of wearable networks, such as finite network topology, ultra-short transmission ranges, space-time radio channel correlations under (biomechanical and behavioural) mobility, etc.

This document, entitled “Demonstration Scenarios and Interfaces between Algorithms and Platforms” (D4.1), summarizes the work carried out in sub-tasks 4.1 and 4.2. This deliverable accounts for two measurement/demonstration campaigns addressing the applicative scenarios specified in task 1. The involved physical demonstrator is composed of *Impulse Radio - Ultra Wideband* (IR-UWB) and *Narrow-Band* (NB) IEEE802.15.4-compliant integrated radio devices, as well as a reference Motion Capture (MoCap) systems delivering the ground truth. The report presents in details the considered physical deployment scenarios and the experimental procedures, showing how they cover motion capture and mobility detection applications on the one hand, as well as single-user and group navigation applications on the other hands. Finally, first post-processing steps necessary to make the measurement/demonstration data fully exploitable in a self-contained database (e.g., post-synchronization of collected radio and MoCap traces), are illustrated within a few representative examples. The produced measurement/demonstration data set will be used to validate localization algorithms and localization-oriented protocol functionalities in the frame of sub-task 4.3. It will also support the development and calibration of physical simulation means in sub-task 2.4.

1. INTRODUCTION

Most of the studies referenced so far in the field of WBAN-based localization have been focusing on measurements based on costly pieces of equipment, either for channel modelling purposes [Cotton14], [Rosini12] or for the validation of on-body localization algorithms based on e.g., impulse radio [Mekonnen10], [Shaban10]. Other approaches aim at characterizing mesh connectivity with integrated narrow-band devices from a pure communication-oriented perspective [Lauzier13]. Finally other works simply rely on simulations and synthetic models [Hamie13], [CORMORAN_D3.1], [CORMORAN_D3.2]. But only rare contributions have considered using real devices to assess the actual performance of on-body nodes localization in large scale contexts, while pointing out critical physical effects related to body mobility.

In the frame of CORMORAN, the sub-task ST4.1 aims at defining demonstration scenarios based on cooperative Wireless Body Area Networks (WBAN), which cover the application scenarios specified in sub-task ST1.1 [CORMORAN_D1.1], while complying with the capabilities of available radio platforms. In sub-task ST4.2, we make sure that the data resulting from these measurement campaigns can be interfaced and exploitable by localization algorithms and protocol building blocks developed in the frame of sub-tasks ST3.x (i.e., for quasi real-time or off-line processing). A bunch of the later algorithms will thus be evaluated and demonstrated in sub-task ST4.3, based on the measurement data issued at real devices. It is also intended to support the efforts made in sub-task ST2.4 towards the development of a WBAN cross-layer physical simulator.

In this deliverable D4.1, which is related to the work carried out in both sub-tasks ST4.1 and ST4.2, we account for two experimental campaigns based on the CORMORAN physical demonstrator aiming specifically at indoor navigation and body mobility detection applications. These multi-standard campaigns involved IEEE 802.15.4-compliant and Impulse Radio - Ultra Wideband (IR-UWB) integrated radio devices, organized within a full mesh topology over on-body, off-body and even body-to-body. The latter devices can produce peer-to-peer Received Signal Strength Indicators (RSSI) and Round Trip - Time of Flight measurements (RT-ToF) respectively, which can feed ranging, positioning or tracking algorithms. During these campaigns, side infrared motion capture systems were exploited for accurate space/time referencing.

The document is structured as follows. In Section 2, we present the pieces of equipment involved in the two measurement/demonstration campaign, including integrated radio devices and motion capture reference systems. Then Section 3 provides a description of the measurement/demonstration set-ups and investigated scenarios. In Section 4, we report elementary post-processing steps applied onto measurement/demonstration data, as well as the software tools to make the raw collected data exploitable, including the challenging post-synchronization of collected measurement traces. On this occasion, examples of single-link

traces are also provided for illustration and discussion. Finally, we report in the Appendices the log files and meta-data information related to the most extensive second measurement campaign.

2. INVOLVED RADIO DEVICES AND REFERENCE OPTICAL SYSTEMS

2.1. RADIO DEVICES

2.1.1 CEA'S IR-UWB TCR DEVICES

The integrated IR-UWB Low Data Rate - Location and Tracking (LDR-LT) devices shown on Figure 2.1, which were developed at CEA-Leti for Wireless Sensor Network (WSN) applications, operate in the band [4.25, 4.75]GHz and host a complete protocol stack from the physical layer [Lachartre09] up to the localization application layer [Pezzin10]. Relying on internal 1 Giga samples per second (Gsps) sampling and 1/1.5-bit quantization on the one hand, as well as on a Differential Binary Phase Shift Keying (DBPSK) modulation on the other hand, these platforms enable data transmissions at the nominal rate of 350 kbps at up to 40 m in LOS (in typical non-WBAN indoor contexts), while allowing peer-to-peer ranging through Round Trip - Time Of Flight (RT-ToF) with clock drift compensation.

Regarding unitary TOA estimates, the platform performs First Arrival Path (FAP) direct detection (with no cross-correlation operations). The index of the first sample exceeding the threshold is viewed as the TOA estimate in the local Rx observation window. Detection is performed within the fine time resolution of 1 ns, corresponding to the internal sampling capability (i.e. equivalently within the spatial resolution of 30 cm).

The active power consumption, on the order of a few 10s of mW (typically, 10 mW in Tx and 30mW in Rx), is comparable with that of State of the Art technologies foreseen in the WBAN context, such as Bluetooth and ZigBee, but providing additional ranging capabilities.

Besides, fast measurement-oriented software, including simplified Medium Access Control (MAC) and applications, have also been developed and ported for flexible demonstration purposes. In particular, the implemented MAC layer enables a beacon-enabled Time Difference Multiple Access (TDMA) superframe structure, which appears adapted for small-size, finite, coordinated and scheduled mesh networks like in our WBAN context. Figure 2.2 shows the corresponding superframe structure [Bucaille07], [Maman08]. The Beacon Period (BP) is entirely specified by the coordinator, which handles resource allocation and scheduling for the entire network. A slotted Aloha scheme is used in the Contention Access Period (CAP), in order to authorize a reduction of the energy consumption [Bucaille07]. Furthermore, data can be transmitted only during the Contention Free Period (CFP) using Guaranteed Time Slots (GTS) to prevent from collisions and improve the Quality of Service (QoS). Hence, in the nominal mode (i.e. in the absence of aggregation and broadcast), three adjacent GTS are reserved for each peer-to-peer range measurement between two distinct asynchronous devices, applying 3-Way ranging transactions [Maman08].

Unfortunately, the implemented MAC suffers from a few limitations in our specific WBAN localization context. One major problem concerns the refreshment rate that could be achievable for updating the peer-to-peer range estimates (and possibly nodes positions in a decentralized positioning scheme), which is strictly bounded by the kind of retrieved PHY information (i.e. Channel Impulse Responses and/or RT-ToF based range information only), by the superframe periodicity and duration, as well as by the number and size of available ranging GTS per superframe. For practicability purposes in our campaigns (but without loss of generality), the coordinator is external to the body and connected to a Personal Computer (PC) through a serial port for configuration and debug. Moreover, an additional USB link is used as a communication interface between this coordinator and the PC.

These platforms have been involved in the first and second measurement campaigns.

CEA-Leti's IR-UWB TCR platforms	
Operating centre frequency / BW	4.5 GHz / 500MHz
Raw binary data rate	350kbps
Issued PHY radiolocation metrics (per link)	- Channel Impulse Responses (though not used in our experiments) - Timers accounting for intermediary TOA estimates - RT-ToF based range estimates
Measurement refreshment rate (per link)	500ms (range info only) up to 2ns (range & CIR info), both in full mesh with 15 nodes
Overall number of available devices per trial	Up to 14
Scenario involvement	Measurement campaigns 1 & 2 (All the scenarios)

Table 2-1: Summary the main characteristics of CEA-Leti's IR-UWB TCR devices

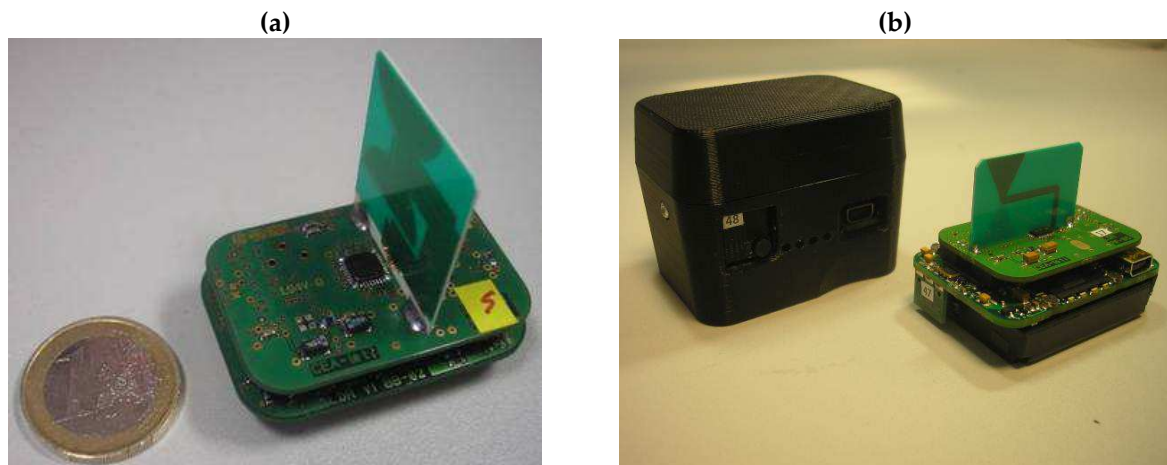


Figure 2.1: CEA-Leti's IR-UWB TCR ranging-enabled device (a-left) besides its package (b-right).

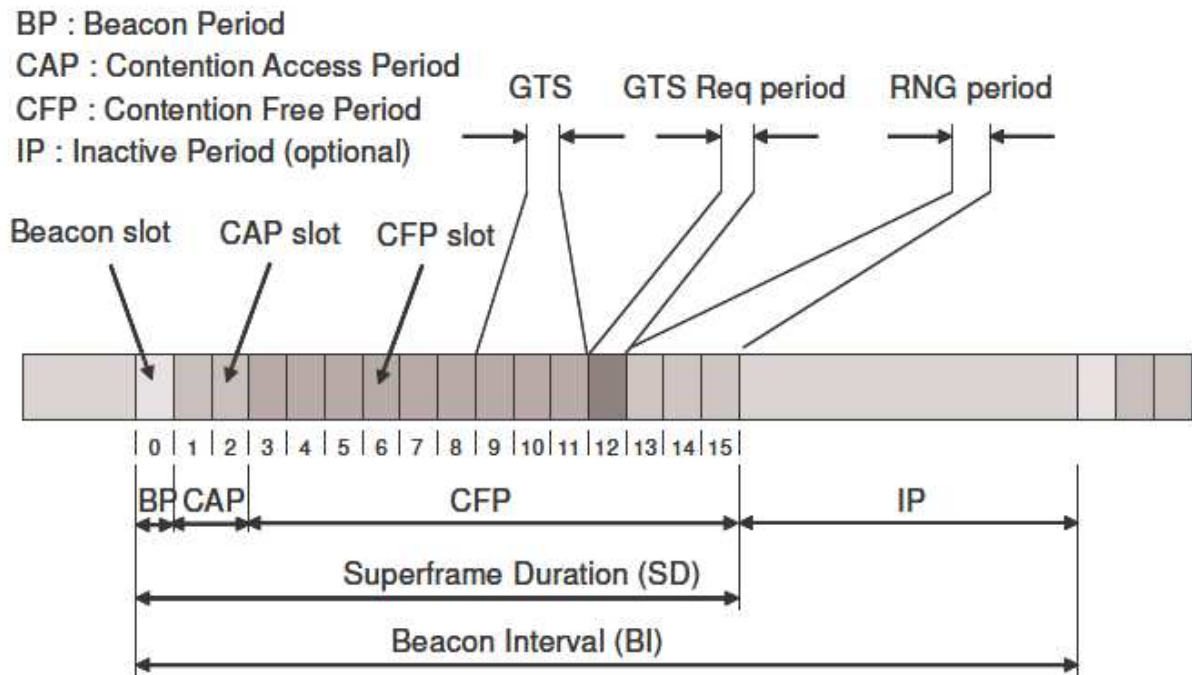


Figure 2.2: Implemented MAC superframe in CEA-Leti's IR-UWB TCR ranging-enabled devices.

2.1.2 BESPOON'S IR-UWB SPOONPHONE AND TAG DEVICES

The BeSpoon company has been developing and integrating high-precision UWB chips in standard smartphones (thus customized as ranging-enabled "Spoonphones" [BeSpoon]) or autonomous battery-powered mobile tags enjoying fine form factor (about a 2-euro coin), as shown on Figure 2.3. Typically, with respect to one particular tag, the SpoonPhone can handle one measurement every 250ms (along with data transmission) at practical ranges spanning between 200 m and 880 m, depending on the chosen antenna and integration sequence. This nominal refreshment period could be scaled down to 125 ms. One given SpoonPhone can monitor up to 6 independent tags. The solution is flexible enough to operate in various authorized bands under the current European regulation for license-free IR-UWB applications, around different central frequencies (namely 3.5GHz, 4GHz, 4.5GHz, in the lower band, and 7.5GHz, 8GHz or 8,5GHz in the upper band), with variable bandwidth (namely from 500MHz to 1GHz). The minimum duration between Rx and Tx consecutive events (at the same device) is about 7.8125 ms, what could be however improved down to a few ms in turn.

These platforms have been involved in the second measurement campaign only.

BeSpoon's IR-UWB SpoonPhone & Tag devices	
Operating centre frequency / BW	3.994 GHz / 1 GHz
Raw binary data rate	N/A (ranging signalling mostly)
Issued PHY radiolocation metrics (per link)	RT-ToF
Measurement refreshment rate (per link)	~ 125 ms (1 master wrt. to 2 nodes, Star)
Overall number of available devices per trial	1 SpoonPhone + 2 mobile Tags
Scenario involvement	Measurement campaign 2 (All the scenarios)

Table 2-2: Summary of the main characteristics of BeSpoon's IR-UWB SpoonPhone & Tags



Figure 2.3: BeSpoon's ranging-enabled "SpoonPhone" and 2 peripheral tags, both hosting IR-UWB "PinPointer" circuits

2.1.3 HIKOB'S IEEE 802.15.4 FOX DEVICES

The involved HiKoB FOX wireless sensors [HikoB], shown on Figure 2.4, embed a processor and a radio chipset whose physical layer is IEEE 802.15.4-compliant in the 2.45GHz ISM band. The FOX radio chipset gives access to the average RSSI obtained over the last 8 received modulation symbols. Similarly to [Lauzier13], a Time Division Multiple Access (TDMA) is considered, each node transmitting periodically in a pre-determined timeslot. An additional longer timeslot is dedicated for logging onto the μ -SD card all the information locally collected by the nodes during each frame. The corresponding protocol adapts the frame duration depending on the number of nodes (e.g. 26ms for 16 nodes).

During this new measurement campaign, up to 12 nodes have been deployed on the subject bodies, whereas 4 more nodes were placed in the immediate environment, serving as fixed anchors.

These platforms have been involved in the second measurement campaign.

HikoB's IEEE 802.15.4 FOX devices	
Operating centre frequency / BW	2.4 GHz
Raw binary data rate	250 kbps
Issued PHY radiolocation metrics (per link)	RSSI
Measurement refreshment rate (per link)	13 ms for 7 nodes/26 ms of 16 nodes (full mesh)
Overall number of available devices per trial	Up to 16
Scenario involvement	Measurement campaign 2 (All the scenarios)

Table 2-3: Summary of the main characteristics of INSA's IEEE 802.15.4 HikoB devices



Figure 2.4: HikoB's IEEE 802.15.4 FOX platforms

2.2. OPTICAL CAPTURE SYSTEMS & VIDEO MEANS

2.2.1 CODAMOTION

In the first measurement campaign, TOA-based range measurements issued at IR-UWB platforms are compared with side reference measurements obtained with the optical CodaMotion tracking system [CodaMotion] (Figure 2.5), which is able to provide very high localization accuracy (i.e. in the order of 0.05 mm) but in very reduced geographical area (on the order of a few m²). Considering the two levels of precisions, the CodaMotion system is used to determine the ranging errors with respect to ground-truth. Hence, one optical marker was placed on each on-body device, in order to define its occupied position in real-time. The data files are fully traceable using legacy formats such as ASCII text.

This system has been utilized only in the first measurement campaign.

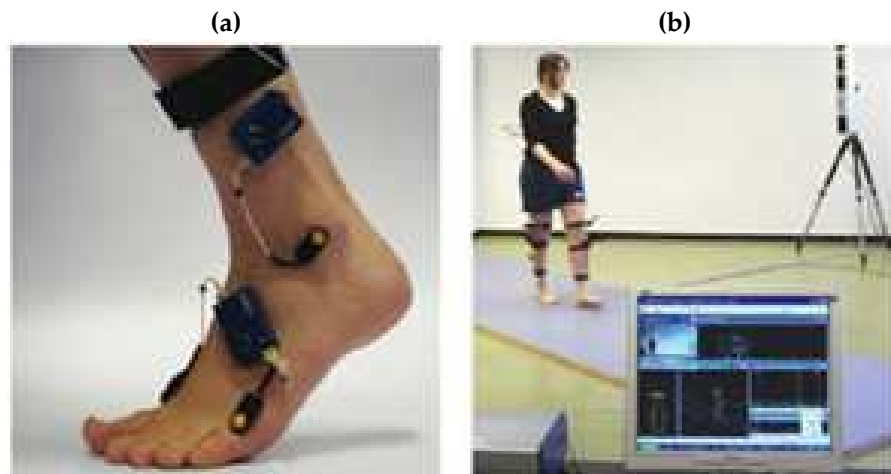


Figure 2.5: “CodaMotion” optical acquisition & tracking system, delivering the reference location information for WBAN-based MoCap applications in the first measurement campaign.

2.2.2 VICON

The Oxford Metrics Group’s Vicon motion capture system, traditionally used to analyse elite athletes’ movements [Bideau10] (See Figure 2.6), was involved in our measurement campaign. In particular, it was used to deliver high-precision spatial referencing (i.e. seen as ground truth), accurate synchronization and mobility modelling for the deployed on-body nodes. The Vicon capture was performed at 100 Hz using 12 infrared cameras surrounding the scene. In each experiment, we equipped the test subject with several tens of markers placed on the on-body devices and on anatomical landmarks to precisely reconstruct each body parts 3D position and orientation. The acquired information is used in the following to compute the exact distances separating the radio nodes and determine radio obstructions at any time.



Figure 2.6: “Vicon” optical acquisition & tracking system (example of capture), delivering the reference location information for WBAN-based MoCap and navigation applications in the second measurement campaign.

3. EXPERIMENTAL SET-UP AND SCENARIOS

3.1. FIRST MEASUREMENT/DEMONSTRATION CAMPAIGN

This first measurement campaign was intended for first qualitative validations of the IR-UWB “TCR” technology, mostly in the context of static MoCap. Various data sets of on-body and off-body range measurements have been collected for different body attitudes and georeferenced with the CodaMotion acquisition system. These measurements enable to verify the modelling hypotheses put forward in [Hamie13b] regarding conditional single-link errors based on IR-UWB TOA estimation. These experiments have been also used for preliminary single-link calibration purposes (out of raw measurements, in the Least Square perspective). Hereafter, the so-called observed range measurements correspond to the calibrated measurements.

The intra-WBAN full mesh topology was also exploited to collect on-body range measurements (including real packet losses due to body shadowing) for relative MoCap in a body-strapped Local Coordinate System (LCS). Based on this data set, D4.2 will for instance account for positioning results, after applying the Constrained Distributed Weighted Multidimensional Scaling (CDWMDS) algorithm described in [CORMORAN_D3.2].

Details regarding the exploitation of the collected measurement data can be found in [Hamie14].

3.1.1 TEST ENVIRONMENT

For the different sub-scenarios and series of this first campaign, measurements were collected in a 4m x 4m office room at CEA-Leti premises, Minatec, Grenoble, France. This confined indoor environment was chosen on purpose for generating dense multipath components with relatively short excess delays.

3.1.2 SCENARIOS

- *Ranging Over On-body and Off-body Single Links (S1.1-S1.6)*

The first set of measurements is performed by placing two IR-UWB “TCR” devices respectively on the chest and the wrist of a static human body in LOS visibility of each other. Measurements have been collected by a time step of 1 sec. Figure 3.1 shows the implemented scenario, depicted in the following as Scenario 1.1. Figure 3.2 plots and compares the successive range measurements with respect to the real distance (delivered by the CodaMotion) between the involved devices over a snapshot time window of 20 sec for illustration purposes. The mean and deviation of ranging errors in this case are respectively equal to 4.7 cm and 16 cm.



Figure 3.1: Experimental Scenario 1.1: On-body ranging over a static chest-wrist link in direct LOS visibility.

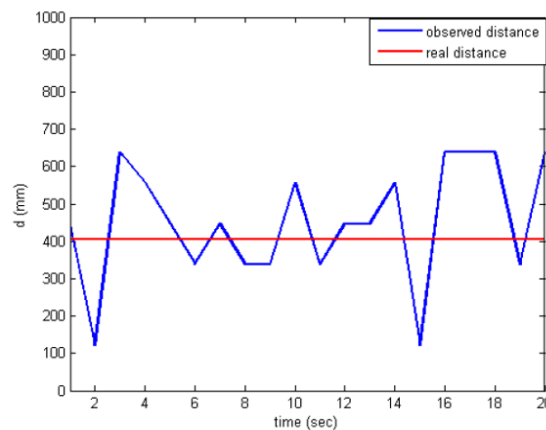


Figure 3.2: Comparison between measured and real distances over the static chest-wrist link in Scenario 1.1 (Ex. of snapshot over 20 sec).

Still considering the chest-wrist link, 3 other sets of measurements have been performed in the so-called Scenarios 1.2, 1.3 and 1.4. Figure 3.3 shows the corresponding body attitudes, which are defined by the wrist position. Table 3.1 summarizes the obtained ranging error parameters for each scenario. The on-body ranging performance achieved in LOS visibility thus seems in compliance with the results presented in [Pezzin10] for classical “body-free” LOS configurations at larger ranges in a typical indoor environment, showing that the standard deviation of ranging errors is relatively stable below 30 cm. Moreover, the observed mean error is relatively small in comparison with the standard deviation and even with the true distance value. Thus, it could be neglected in first approximation over on-body links in direct LOS visibility. Those observations tend to confirm the zero-mean Gaussian hypothesis retained in [Hamie13] for IR-UWB TOA-based on-body measurements in LOS. However, the standard deviation observed with the real platforms is significantly larger than that initially based on channel sounding measurements [Hamie13] (i.e. previously on the order of 10 cm in favorable Signal to Noise Ratio (SNR) conditions) and hence, larger than the values assumed in the simulations of e.g., [Hamie12]. This degraded accuracy is mostly due to the direct sample FAP detection scheme implemented in the real IR-UWB platforms, given the finest temporal granularity of 1 ns, whereas in [Hamie13], the performance was bounded by larger signal bandwidths and the resulting resolution capability (i.e. assuming an ideal and quasi-infinite temporal granularity at the receiver).



Figure 3.3: Experimental Scenarios 1.2 (left), 1.3 (middle) and 1.4 (right): On-body ranging over the chest-wrist link in direct LOS visibility, for different body attitudes.

	Error Std (cm)	Mean Error (cm)
Scenario 1.1	16	4.7
Scenario 1.2	22	-4
Scenario 1.3	21	3
Scenario 1.4	24	5

Table 3-1: On-Body TOA-based ranging error parameters in Scenarios 1.1 to 1.4

The ranging error is now evaluated over static on-body links in systematic NLOS configurations (i.e. under strong body shadowing). Two IR-UWB devices have been placed on the chest and the back of the subject body. Figure 3.4 (left) shows the implemented scenario, depicted as Scenario 1.5 in the following. Similarly to the previous sets, the range measurements have been collected by a time step of 1 sec. Figure 3.5 (left) shows an example

of snapshot window for 20 sec, comparing the observed range measurements with the real distance. The mean and standard deviation of ranging errors are respectively equal to 5.68 m and 78 cm in this case, what may be redhibitory to the localization system. This phenomenon is likely due to a missed detection of the direct path, where TOA estimation adversely relies on a late secondary path, which may be reflected or diffracted by the surrounding materials (e.g. distant wall, distant metallic pieces of furniture), and hence, the length of the detected path is significantly biased from the direct one. One more complementary remark is that the devices' placements tend to limit also the sensitivity to close reflections (e.g. typically single-bounce reflections on the ground) due to severe body obstructions also along the vertical dimension, what is most likely combined with penalizing relative antenna orientations. The propagation of radio waves diffracted around the body seems to be excluded as well in this case. The phenomenon is anyway all the more pessimistic in comparison with the results from [Hamie13] since no temporal restriction of the Rx observation window (i.e. in terms of excess delay) is applied while estimating TOA in the IR-UWB platforms (i.e. contrarily to the 5 ns window restriction assumed in [Hamie13] with respect to the temporal synchronization point, hence taken into account the finite -and even confined-WBAN spatial dimensions).



Figure 3.4: Experimental Scenarios 1.5 (left), 1.6 (right): On-body ranging over static chest-back and chest-wrist links respectively, under systematic NLOS conditions.

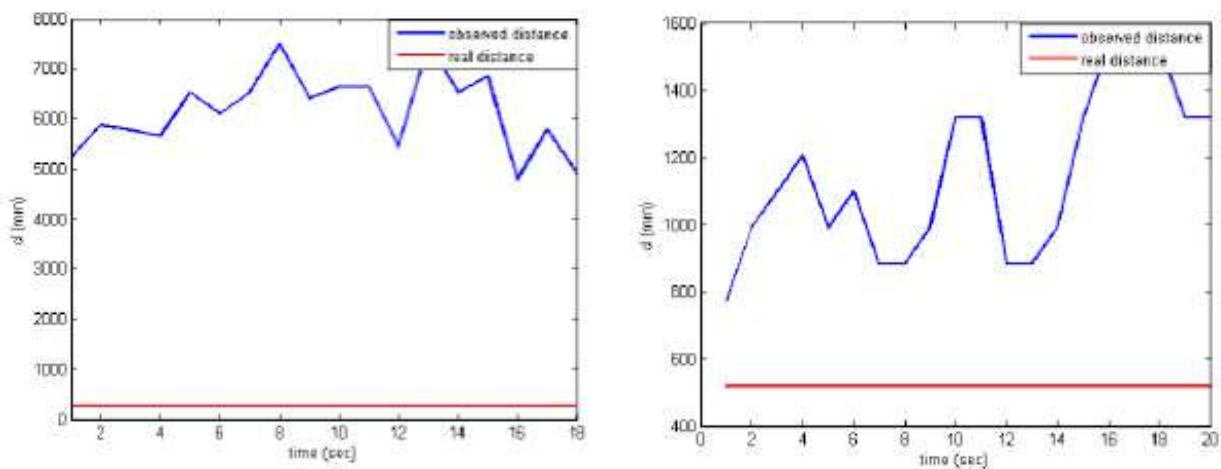


Figure 3.5: Comparison between measured and real distances over the chest-back and chest-wrist links in Scenarios 1.5 and 1.6 respectively.

In Scenario 1.6, the chest-wrist link has been considered, for being partially obstructed by human body shadowing (i.e. comprising also an unobstructed portion over-the-air), just like the link characterized in [Hamie13]. Figure 3.4 (right) shows the corresponding scenario configuration, whereas Figure 3.5 (right) illustrates a comparison between the observed range measurements and the real distance separating the involved devices within a snapshot window of 20 sec by a time step of 1 sec. The range measurement is again positively biased, with a mean error of 62 cm and a standard deviation of 25 cm. Like in Scenario 5, the positive bias is due to the detection of a late reflected path, but most likely resulting from a less distant interaction with the environment. This makes the use of partially obstructed links (like this chest-wrist link) much more tractable for localization purposes. Moreover, the idea of positively biased range measurements over NLOS on-body links is compliant with the model defined in [Hamie13], all except but the order of magnitude of this bias, which again depends on the kind of obstruction (i.e. full or partial) and Rx device capabilities (i.e. restriction of the Rx observation window, time granularity, antenna pattern and placement).

In order to evaluate also the ranging errors over off-body links (mostly for comparison purposes), we take benefit from Scenario 1.5, using the chest-placed device in direct LOS visibility with the coordinator attached to the storing PC, which is external to the body and located in the surrounding environment. On the other hand, the back-placed device is under systematic NLOS conditions from the same coordinator. Figure 3.6 (left) plots and compares the measured distances with respect to the real distance over the considered LOS off-body link (i.e. chest-coordinator). In this case, the mean ranging error is 5.6 cm and the standard deviation 17 cm. These results are compliant with the ranging error parameters observed over LOS on-body links. Figure 3.6 (right) shows similar results over the considered NLOS off-body link, whose range measurements are again positively biased, with a mean error of 2.08 m and a standard deviation of 23 cm, that is to say, on the same order of magnitude in comparison with strong NLOS on-body configurations (e.g. chest-back).

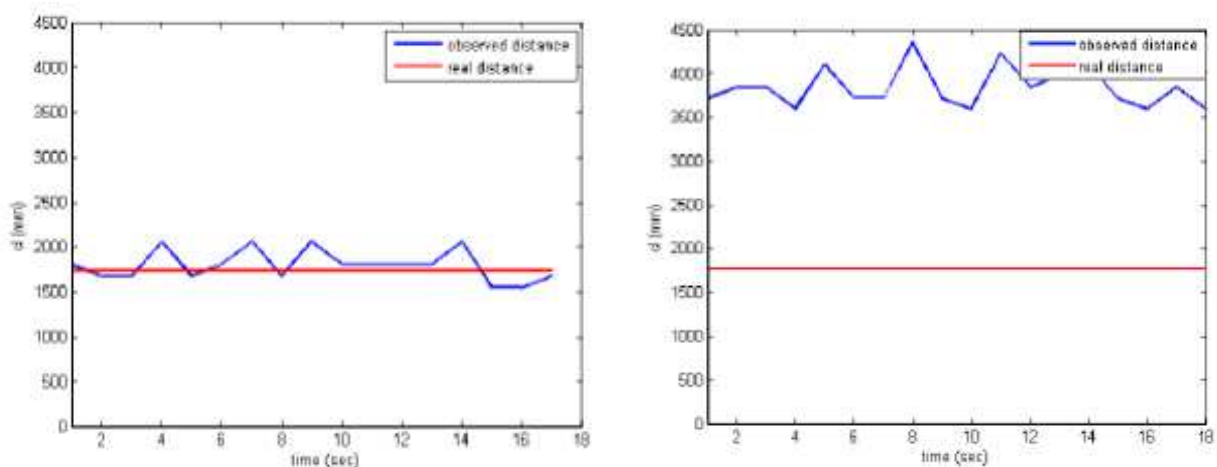


Figure 3.6: Comparison between measured and real distances over the chest-coordinator (left) and back-coordinator (right) off-body links respectively (with the subject facing the coordinator), under LOS and NLOS conditions respectively (mutualized with Scenario 1.5).

- *Small-Scale Individual Motion Capture (S1.7)*

In this section, we account for other experiments addressing relative MoCap applications based on the previous on-body range measurements. For this sake, a full on-body mesh topology is considered, including 10 devices, as shown on Figure 3.7. Devices 1 to 4 are considered as on-body anchors that define a stable Cartesian LCS, which remains unchanged and time-invariant under body mobility. The remaining devices are considered as simple on-body nodes to be positioned. Table 3.2 summarizes the positions occupied by those devices, along with their status (i.e. simple mobile node or on-body anchor).

Device ID	On-body Position	Category
1	Chest	On-body anchor
2	Chest	On-body anchor
3	Left hip	On-body anchor
4	Back	On-body anchor
5	Right shoulder	On-body node
6	Right elbow	On-body node
7	Right wrist	On-body node
8	Left shoulder	On-body node
9	Left elbow	On-body node
10	Left wrist	On-body node

Table 3-2: IDs, positions and categories of the on-body IR-UWB TCR devices used in relative MoCap experiments during the 1st measurement campaign.



Figure 3.7: On-body network deployment scenario for MoCap experiments during the 1st measurement campaign.

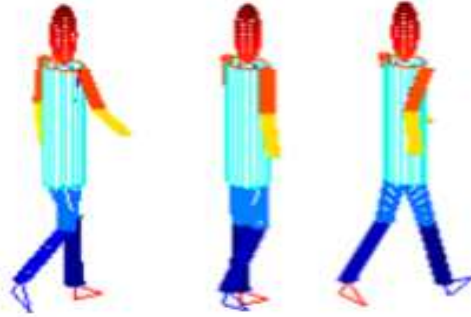


Figure 3.8: Retained body gestures for considering a quasi-dynamic localization problem.

In this measurement setup, we had to face difficulties in synchronizing the CodaMotion tracking system and the involved IR-UWB devices in case of truly dynamic scenarios. To overcome this problem, we defined 3 static body postures corresponding to three key phases of the walk cycle. Range measurements have been collected in each posture for periods of 10 sec by the same time step of 1 sec, as previously. Figure 3.8 shows successive snapshots of the retained body gestures, based on a biomechanical model representation used in [Hamie12]. The idea was to emulate mobility afterwards, assuming that a real body under moderate walk would switch between the last 3 gestures, taking approximately 1 sec between two adjacent gestures.

3.2. SECOND MEASUREMENT / DEMONSTRATION CAMPAIGN

This new multi-standard campaign was set-up for multiple purposes: comparison of different collocated technologies under similar deployment conditions, calibration of deterministic simulation tools developed in ST2.4, off-line validation of localization algorithms put forward in ST3.2, preparation to the performance evaluation of CORMORAN demonstrator in ST4.3, creation of an unprecedented WBAN measurement database fed with real cooperative data issued at integrated devices. Details concerning the early exploitation of collected measurement data can be found in [Denis14].

3.2.1 TEST ENVIRONMENT

This second set of experiments was realized in a gymnasium usually dedicated to motion capture studies at ENS/IRISA Cachan Bretagne, France (« Immermove » platform, counting among the most significant facilities in Europe in this research community). The capture zone was restricted to a 13mx8m area, including the 4 anchors and surrounded by the Vicon infrastructure (See Figure 3.9, Figure 3.10 and Figure 3.12). Even if it could not perfectly reproduce real multipath effects that would be observed in a more conventional indoor context (e.g., in terms of excess delay), this environment enables larger-scale body mobility in an open space (in comparison with the first measurement campaign), and thus, it enables to capture realistic dominating body shadowing effects (in both single-user and group configurations).



Figure 3.9: Panoramic view of the test environment in the second measurement campaign.

3.2.2 SCENARIOS

For both IR-UWB TCR and IEEE 802.15.4 HikoB FOX technologies, respectively up to 11 and 12 mobile nodes were deployed on the subject bodi(es) (See Figure 3.11), whereas 4 more nodes were placed in the immediate environment, serving as fixed anchors of infrastructure, (Access Points) AP_i , $i = 1...4$, at 1.06m of height (See Figure 3.10). Depending on the underlying application, the mobile on-body devices are either concentrated on one single carrying body (mobility detection, motion capture and single-user navigation...) or distributed over three carrying bodies (group navigation). As for the IR-UWB BeSpoon technology, a SpoonPhone was carried in the right hand of one equipped subject (to mimic the use of a conventional handset device for navigation display), whereas 2 tags were deployed either as anchors in navigation scenarios (i.e., physically collocated with that of IR-UWB and IEEE 802.15.4 technologies) or mounted on one shoe and the opposite hand in mobility detection and motion capture scenarios.

The scenarios of this second measurement campaign deliberately mixed moderate pedestrian walking and static poses (for mobility and attitude detection), each trial lasting for about 110 sec. At the beginning of each acquisition, a specific arm gesture was made by the main subject so as to synchronize motion capture and radio sub-systems (See post-synchronization procedure in section 4.1).

For single-user scenarios, the subject body was standing right in the middle of the scene, facing each anchor for approximately 5 sec each and rotating over the 4 anchors sequentially. For the sake of illustration, Figure 3.10 reports time-stamped snapshots of the body posture and orientation at different instants (corresponding to the 9 sequences), spanning from $t = 0$ sec till $t = 90$ sec, in a trial where the subject started moving at time $t = 20$ sec along a rectangular trajectory centered on the starting point. The full sequence is divided into 9 moving sub-sequences, where the subject walks from one point of interest to another, with 9 intercalated static sequences.

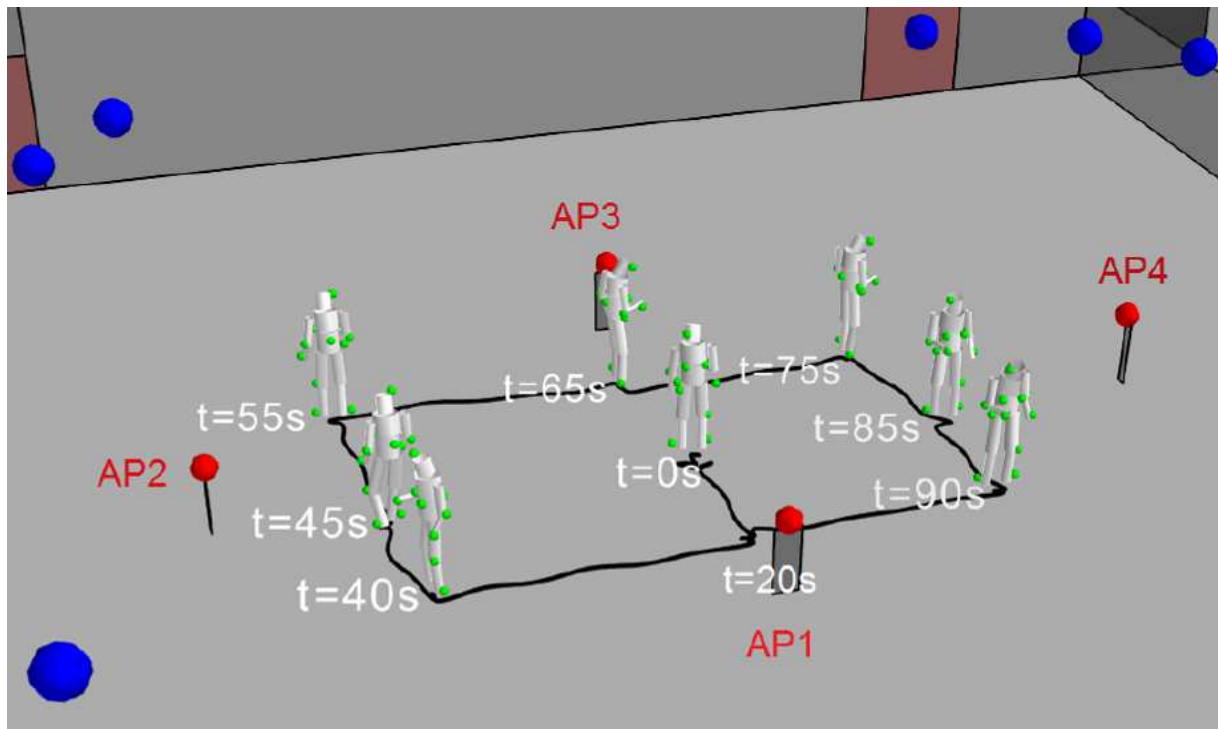


Figure 3.10: Partial view of deployment scenario in single-user experiments, including 4 fixed anchors (red spheres), 12 infrared cameras (big blue spheres), the followed trajectory (black ground path), and time-stamped snapshots of the body poses (articulated chains of light grey cylinders captured with the reference Vicon system) with on-body radio nodes (green spheres) for LSIMC.

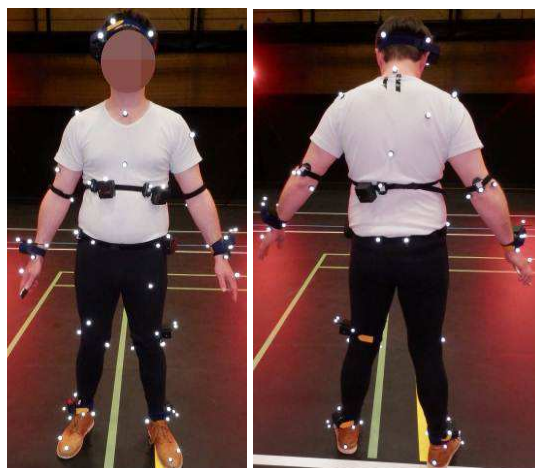


Figure 3.11: Front and back pictures of the equipped subject, including 12 on-body IEEE 802.15.4 HikoB FOX nodes and 10 IR-UWB TCR nodes, along with several tens of Vicon markers in single-user LSIMC scenarios.

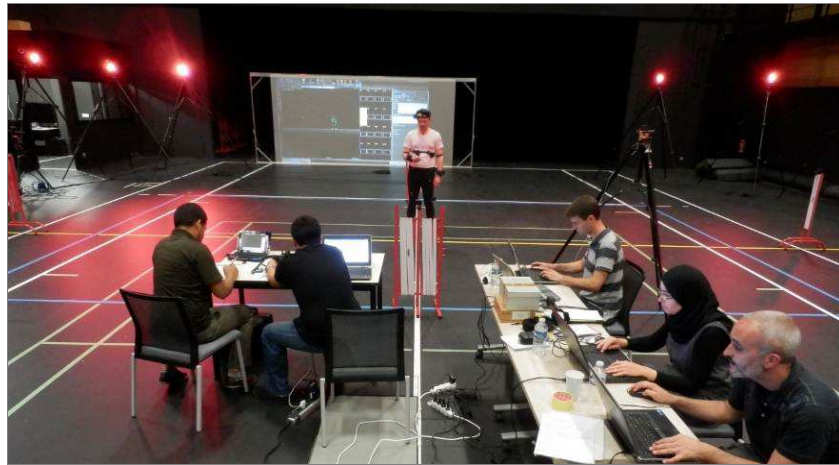


Figure 3.12: CORMORAN team operating during one single-user acquisition of the second measurement campaign, with 5 of the 12 infrared Vicon cameras (red lights) surrounding the scene.

- *In-Site Calibration & Functional Validation (S2.0)*

This very first scenario was mostly intended for the functional validation of each on-body technology, assessing possible co-existence and/or coupling issues between the different on-body nodes (and possibly, between the different technologies), and verifying the validity of the collected data. Several distinct runs were launched for each deployment configuration (i.e., IEEE 802.15.4 HikoB FOX and IR-UWB BeSpoon Spoonphone & tags on the one hand, IR-UWB TCR on the other hand).

The corresponding series of Day 1 (i.e., reference Vicon file number) are reported as 1 to 4 for TCR devices, and 5 to 8 (& 31) for HikoB and BeSpoon devices.

- *Large-Scale Individual Motion Capture (S2.1x)*

In the following scenarios, we consider one single user carrying ~10 on-body nodes and 4 fixed elements of infrastructure surrounding the scene, under moderate pedestrian walk (S2.1a) (also exploitable for single-user navigation), a succession of static and dynamic Yoga postures (also exploitable for attitude/posture classification/learning/detection) (S2.1b and S2.1e respectively), a succession of dynamic Kung Fu gestures (S2.1c), and a succession of usual daily-life gestures (S2.1d).

Scenario 2.1a

- **Overall synopsis** - 1 min 30 sec
 - Self-rotation of the subject at the center of the scene (clockwise)
 - 1min of moderate walk along a pre-defined path on the floor, including
 - ~30 sec with the SpoonPhone in the hand ahead (emulating situations with a display handset and varying the on-body shadowing conditions);

- ~30 sec with the SpoonPhone in the hand, but not necessarily hold ahead in front of the carrying body carrier (thus emulating the natural balancing of the arms during the walk cycle);
- ~30 sec of accelerated walk (till moderate run)
- **Deployment**
 - Radio devices
 - BeSpoon's SpoonPhone and Tags:
 - 1 SpoonPhone hold in the right hand of the subject
 - 1 mobile tag at the left wrist (~ emulating a smart watch)
 - 1 mobile tag on the right ankle (~ emulating a smart shoe)
 - CEA's TCR :
 - 10 on-body nodes
 - Head right
 - Torso right
 - Torso left
 - Back center
 - Hip right
 - Wrist right
 - Wrist left
 - Knee left
 - Ankle right
 - Ankle left
 - 4 external anchors (including the coordinator)
 - HikoB's FOX :
 - 12 on-body nodes
 - Head right
 - Torso right
 - Torso left
 - Back center
 - Elbow right
 - Elbow left
 - Hip right
 - Wrist right
 - Wrist left
 - Knee right
 - Knee left
 - Ankle right
 - Ankle left

- Optical Vicon's tags
 - Tags collocated with on-body radio devices (e.g., 12 with HikoB's FOX on-body nodes & 3 with BeSpoon's SpoonPhone and 2 Tags)
 - Remaining tags are disseminated on the body, according to MoCap needs and/or post-simulation needs (e.g., cylinders diameters in UR1 PyLayers deterministic simulations while animating the biomechanical mobility model)

Figure 3.13 below shows the physical deployment scenario S2.1a (similar to that of scenarios S2.1b and S2.1c).

The corresponding series of Day 1 (i.e., reference Vicon file number) are numbered as 9 to 12 for TCR devices, 13 to 16 for HikoB and BeSpoon devices and finally, 32 to 35 for the three radio technologies simultaneously (with collocated HikoB and TCR devices).

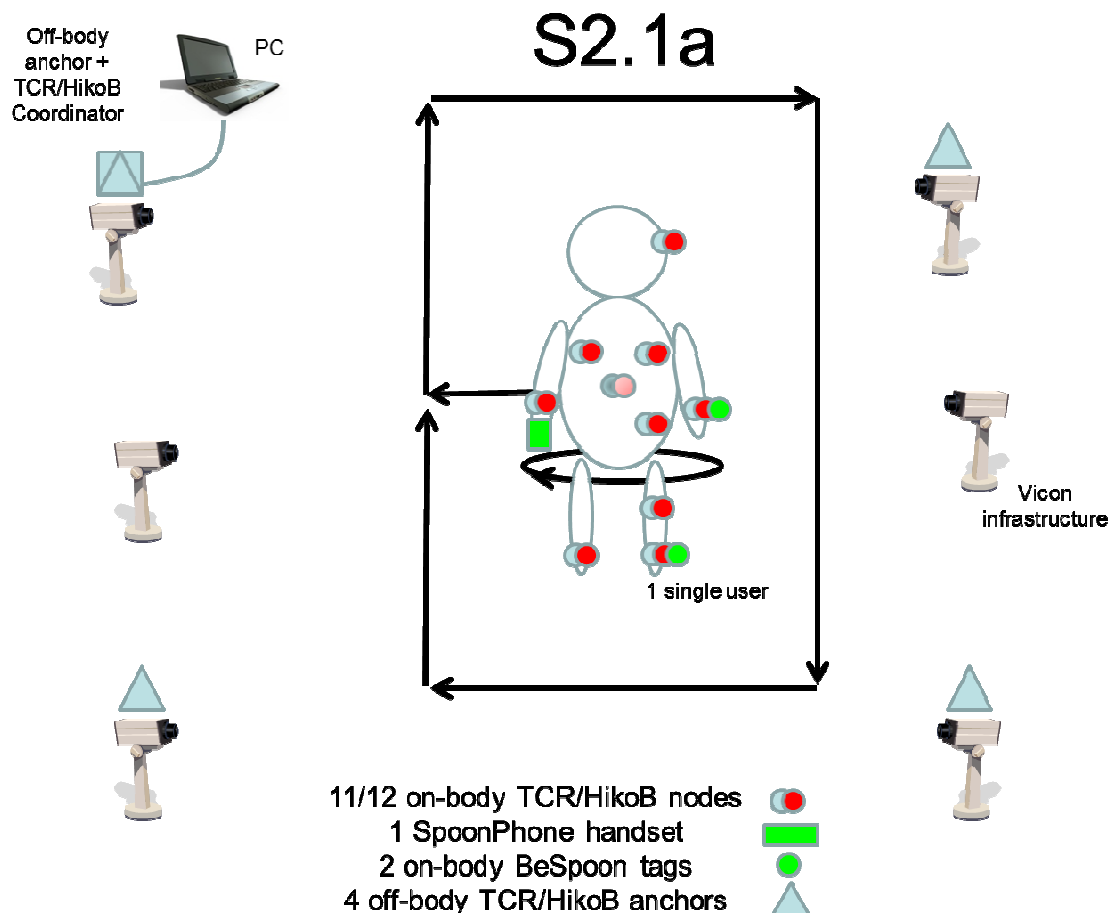


Figure 3.13: Deployment scenario for scenario S2.1a (LSIMC) under moderate walk (single user) (Similar deployment for scenarios S2.1b and S2.1c).

Scenario 2.1b

- **Overall synopsis**
 - 1 single subject body at the center of the scene
 - Succession of static canonical postures (Yoga), each for ~10 sec
- **Deployment**
 - Similar to S2.1a

The corresponding series of Day 1 (i.e., reference Vicon file number) are numbered as 17 to 20 for TCR devices and 21 to 24 for HikoB and BeSpoon devices.

Scenario 2.1c

- **Overall synopsis**
 - 1 single subject body at the center of the scene
 - Succession of slow dynamic gestures (Kung Fu)
- **Deployment**
 - Similar to S2.1a

The corresponding series of Day 1 (i.e., reference Vicon file number) are numbered as 25 to 26 for TCR devices and 21 to 24 for TCR devices only.

Scenario 2.1d

- **Overall synopsis**
 - 1 single subject body moving erratically on the scene
 - Succession of natural dynamic daily-life gestures (e.g., sitting and standing on a chair, opening and closing a door...)
- **Deployment**
 - Similar to S2.1a

The corresponding series of Day 1 (i.e., reference Vicon file number) are numbered as 27 to 28 for HikoB and BeSpoon devices only.

Scenario 2.1e

- **Overall synopsis**
 - 1 single subject body at the center of the scene
 - Succession of slow dynamic postures (Yoga)
- **Deployment**
 - Similar to S2.1a

The corresponding series of Day 1 (i.e., reference Vicon file number) are numbered as 29 to 30 for HikoB and BeSpoon devices only.

- *Group Navigation Scenarios (S2.2x)*

In the following scenarios, we consider several equipped users, each carrying 2 or 3 on-body nodes and 4 fixed elements of infrastructure surrounding the scene, under moderate grouped/coordinated progression (e.g., firemen, soldiers...) followed by grouped jogging (S2.2a), and random multi-user walk with gradually increased crowd density (S2.2b).

Scenario 2.2a

- **Overall Synopsis**
 - 3 mobile equipped subject bodies
 - 1 round of coordinated walk/progression (e.g., firemen, soldiers...), followed by 2 rounds in grouped jogging, both along the pre-defined path on the floor
- **Deployment**
 - Radio
 - BeSpoon's SpoonPhone and Tags:
 - SpoonPhone hold in the right hand of one subject
 - 2 external tags as anchors (collocated with 2 of the TCR/FOX anchors)
 - CEA's TCR :
 - 11 on-body nodes distributed over the 3 body subjects, comprising 3 to 4 nodes for each body
 - 1 on the torso right
 - 0 (1 subject only) to 1 (2 subjects) on the torso left
 - 1 on the shoulder left
 - 1 on the back center
 - 4 external anchors (like in Scenarios 1.x)
 - HikoB's FOX:
 - 12 on-body nodes distributed over the 3 body subjects, comprising 3 to 4 nodes for each body
 - 1 on the torso right
 - 1 on the torso left
 - 1 on the shoulder left
 - 1 on the back center
 - 4 external anchors (like in Scenarios 1.x)
 - Vicon's optical tags
 - Tags collocated with on-body radio devices (e.g., 12 with HikoB's FOX on-body nodes & 3 with BeSpoon's SpoonPhone and 2 Tags)
 - Remaining tags are disseminated on the body, according to MoCap needs and/or post-simulation needs (e.g., cylinders diameters in UR1 PyLayers deterministic)

simulations while animating the biomechanical mobility model)

Figure 3.14 below shows the physical deployment scenario S2.2a.

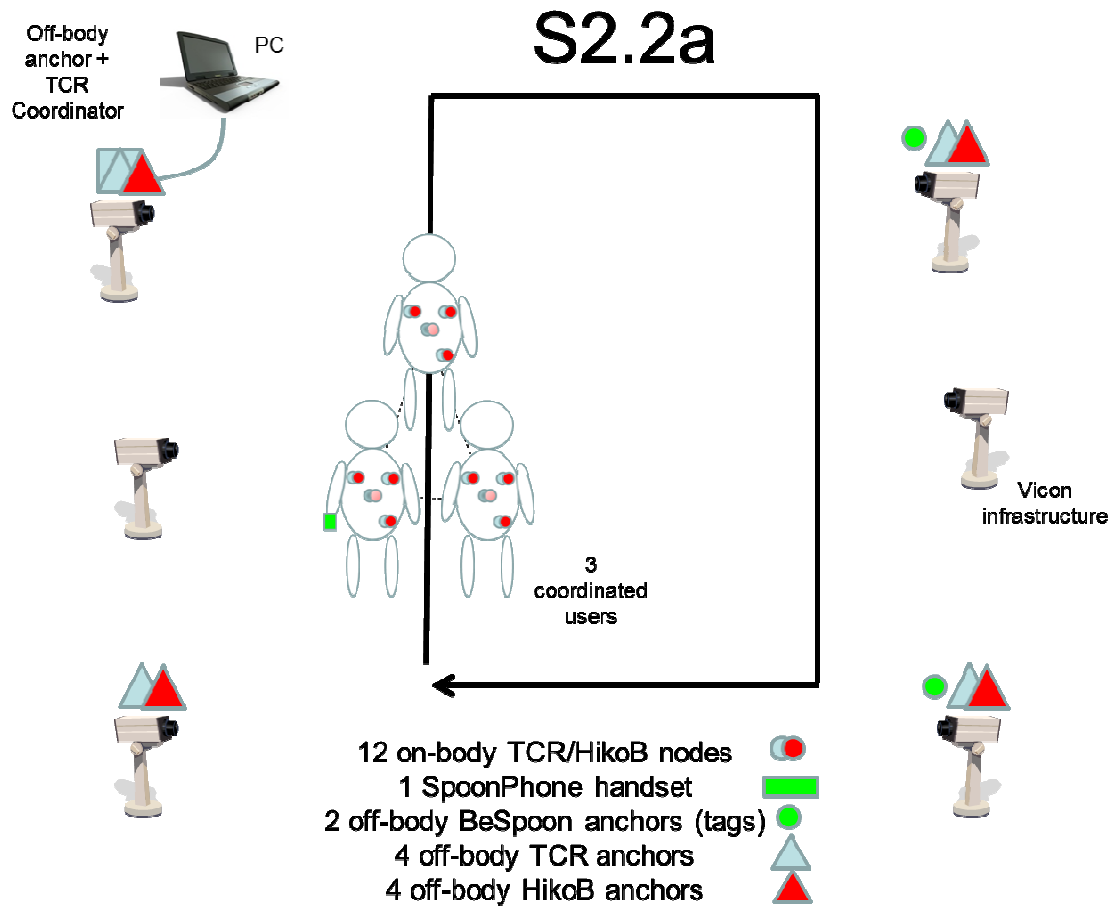


Figure 3.14: Deployment scenario for scenario S2.2a (CGN) (3 users).

The corresponding series of Day 2 (i.e., reference Vicon file number) are numbered as 1 to 4 for TCR devices, 17 to 20 for HikoB and BeSpoon devices and finally 9 to 12 for the three radio technologies simultaneously (with collocated HikoB and TCR devices).

Scenario 2.2b

- **Overall Synopsis**
 - 3 mobile equipped subject bodies, with other mobile non-equipped pedestrians.

- Random walk of the 3 equipped subjects on the scene, with additional pedestrians obstructing the radio Body-to-Body links between equipped users (Emulating gradual human density with 2 more pedestrians per 10 sec).
- **Deployment**
 - Similar to Scenario S2.2a.

Figure 3.15 below shows the physical deployment scenario S2.2b.

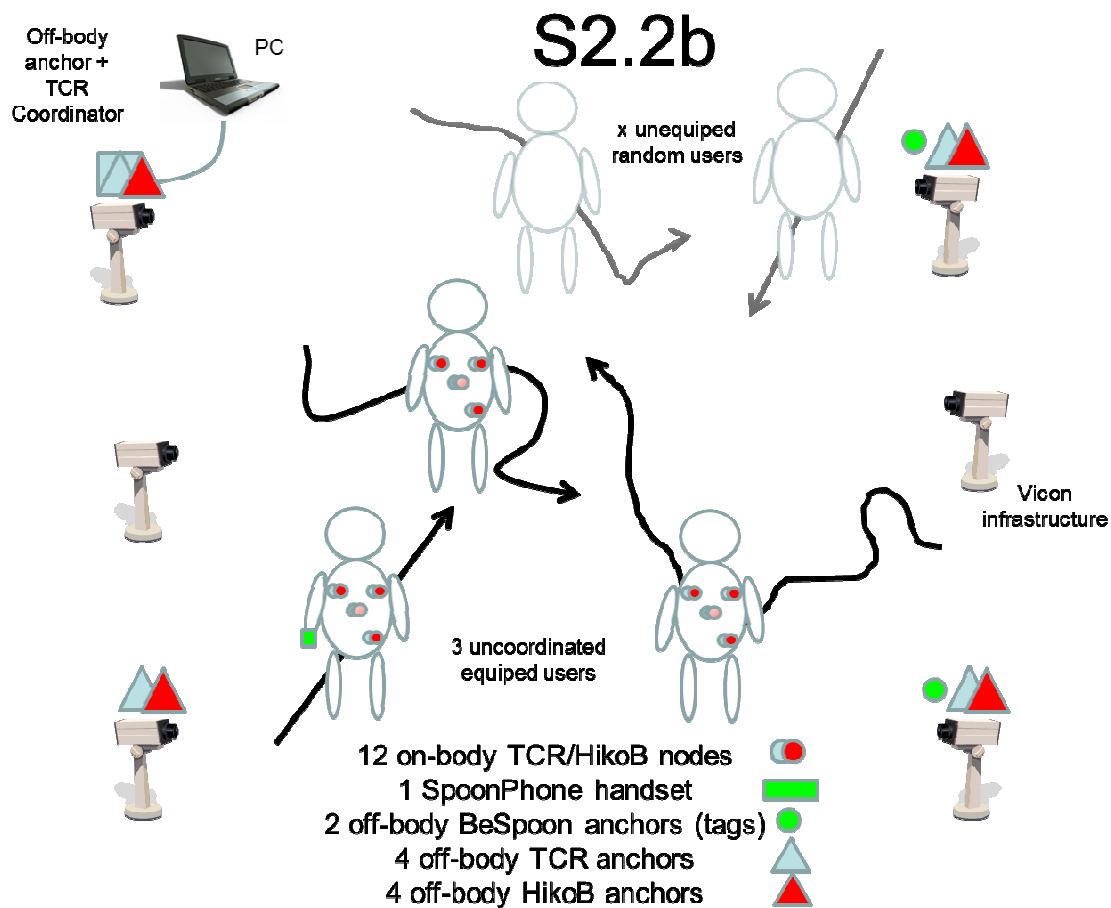


Figure 3.15: Deployment scenario S2.2b - CGN under random walk (3 equipped users) & additional unequipped pedestrians (causing body shadowing over useful off-body and body-to-body links).

The corresponding series of Day 2 (i.e., reference Vicon file number) are numbered as 5 to 8 for TCR devices, 21 to 24 for HikoB and BeSpoon devices and finally 13 to 16 for the three radio technologies simultaneously (with collocated HikoB and TCR devices).

4. FIRST POST-PROCESSING STEPS AND RESULTING MEASUREMENT/DEMONSTRATION DATABASE

In this section, we describe early post-processing steps applied onto raw radio and reference MoCap measurements so as to make the traces exploitable for further processing (e.g., application of localization algorithms from sub-task ST3.2 [CORMORAN_D4.2], deterministic simulations fed with ground-truth and comparison with real radio traces in sub-task ST2.4 [CORMORAN_D2.6]). On this occasion we also introduce the format of the resulting measurement database, the computer tools to manipulate/extract the data, as well as a few examples of collected traces.

Overall the measurement/demonstration data are made publicly available in two different ways: i) either raw data exploitable within a specific software tool in the frame of the PyLayers simulator [PyLayers] for generic custom/extended usage by the research community (e.g., propagation and mobility modelling...) or ii) post-processed and self-contained data accessible from Matlab for direct algorithm evaluation, as reported in CORMORAN's D4.2 [CORMORAN_D4.2].

4.1. POST-SYNCHRONIZATION OF RADIO AND MOCAP TRACES

At the beginning of each trial in the second measurement campaign (on both Days 1 and 2), as mentioned before, a specific procedure has been set-up for post-synchronization purposes between radio devices and the Vicon reference system, as follows:

- Launched acquisitions for all the systems in parallel (i.e., radio and non-radio) based on a coarse oral “top”, with the main subject being static on the scene;
- After a few seconds, specific pre-convincing gesture performed by the main subject (duration on the order of ~ 1 sec) to enable detecting the beginning of the mobility sequence in post-processing. One aim is to compensate the uncertainties -in terms of latency- between the oral “top” and the actual beginnings of acquisition at the different sub-systems.

Thus, so as to make the data exploitable, the challenge of this first post-synchronization step is three-fold:

- Realign all the systems in time at the beginning of the acquired mobility sequence (i.e., delivering a common starting time stamp “T0” on the local timelines) → This is possible e.g., through cross-correlation of radio traces with MoCap-based deterministic predictions;
- Compensate for possible relative clock drifts between the systems;
- Ensure identical and unitary sampling frequency despite different acquisition speeds → This is made possible e.g., through decimation and/or interpolation (by default, the Vicon reference system was the one with the highest refreshment rate). Time bases from MoCap and Hikob have thus been harmonized and have the same sampling rate after post-processing.

For resynchronizing the RSSI and Euclidean distance information coming from the MoCap system, that is to say, to determine the best time shift and sample decimation factor, we have first built a composite quantity **dsh** (accounting for distance and body shadowing) based on the latter MoCap outputs, including both exact distance and link occultation information. It is calculated as the inverse of the squared distance expressed in dB, with an extra constant offset of **15 dB** (optimized empirically) when body shadowing has been detected. This quantity is then centered on the mean value of the RSSI, for comparison purposes.

Figure 4.1 and Figure 4.2 below shows the resulting superposition of the MoCap related information **dsh** defined above and the HIKOB RSSI measurements for different links in the series 6 of scenario SC21.a. The links are sorted according to the decreasing cross-correlation value between the two superposed traces, after applying the time reconciliation procedure. Figure 4.1 shows the 16 most correlated links and Figure 4.2 the 16 less correlated link. This global vision of all the links can give a good idea of the quality of the achieved time resynchronization. Most of the errors come from situations where a LoS condition has been detected whereas the link is strongly engaged. In such situations, more predictive models of the RSSI would achieve better performances. It is also to be noticed that some of the resulting fluctuations observed around the trace built on top of a prior heuristic modeling assumptions (about mobility and body shadowing effects) may be also caused by unfiltered small-scale fading effects (i.e., not completely removed by RSSI averaging).

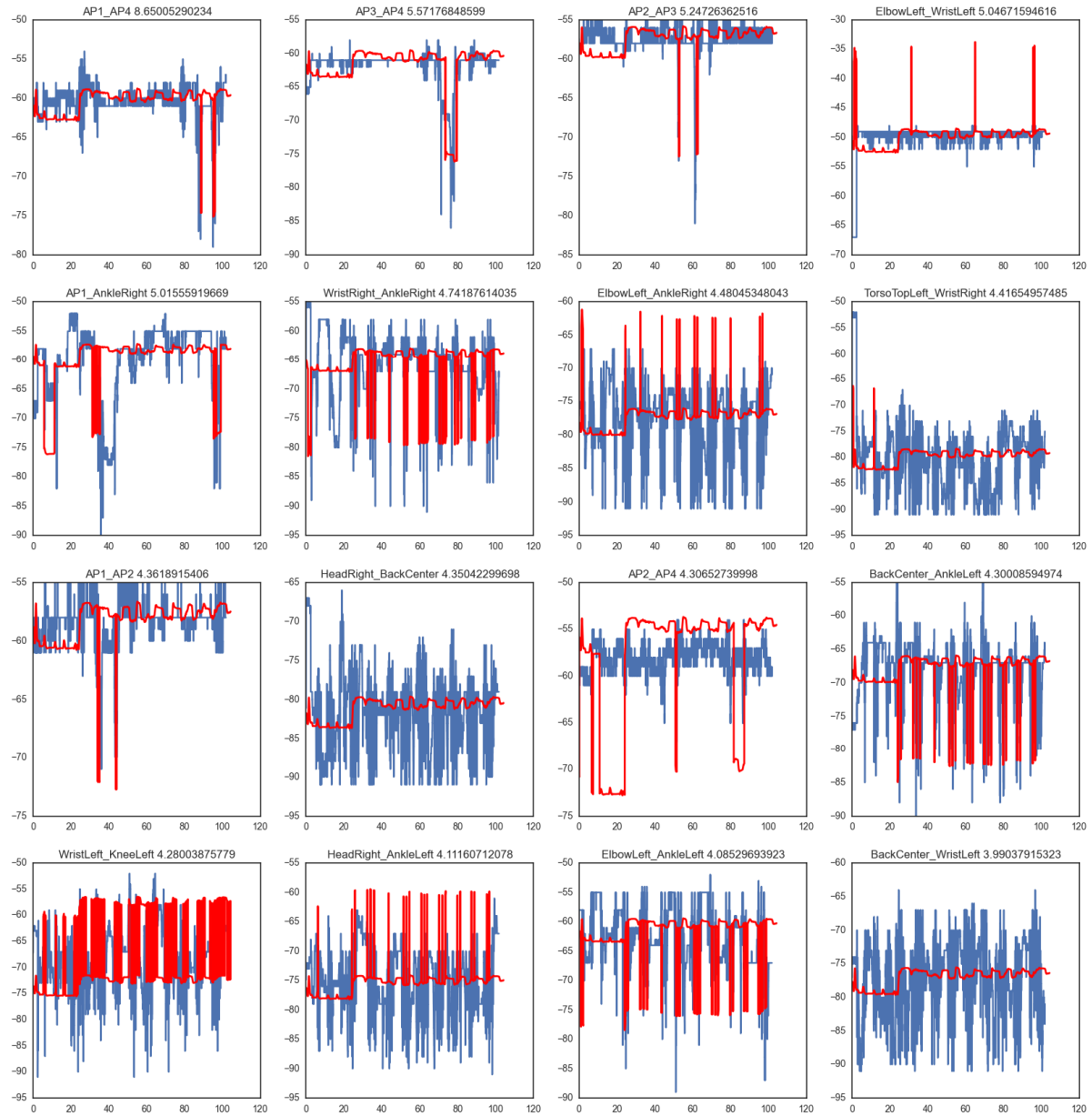


Figure 4.1: Comparison of HKB RSSI vs centered distance shadowing indicator from MoCap (red) time series, 16 sorted most correlated links (Scenario Sc21.a, Series 6).

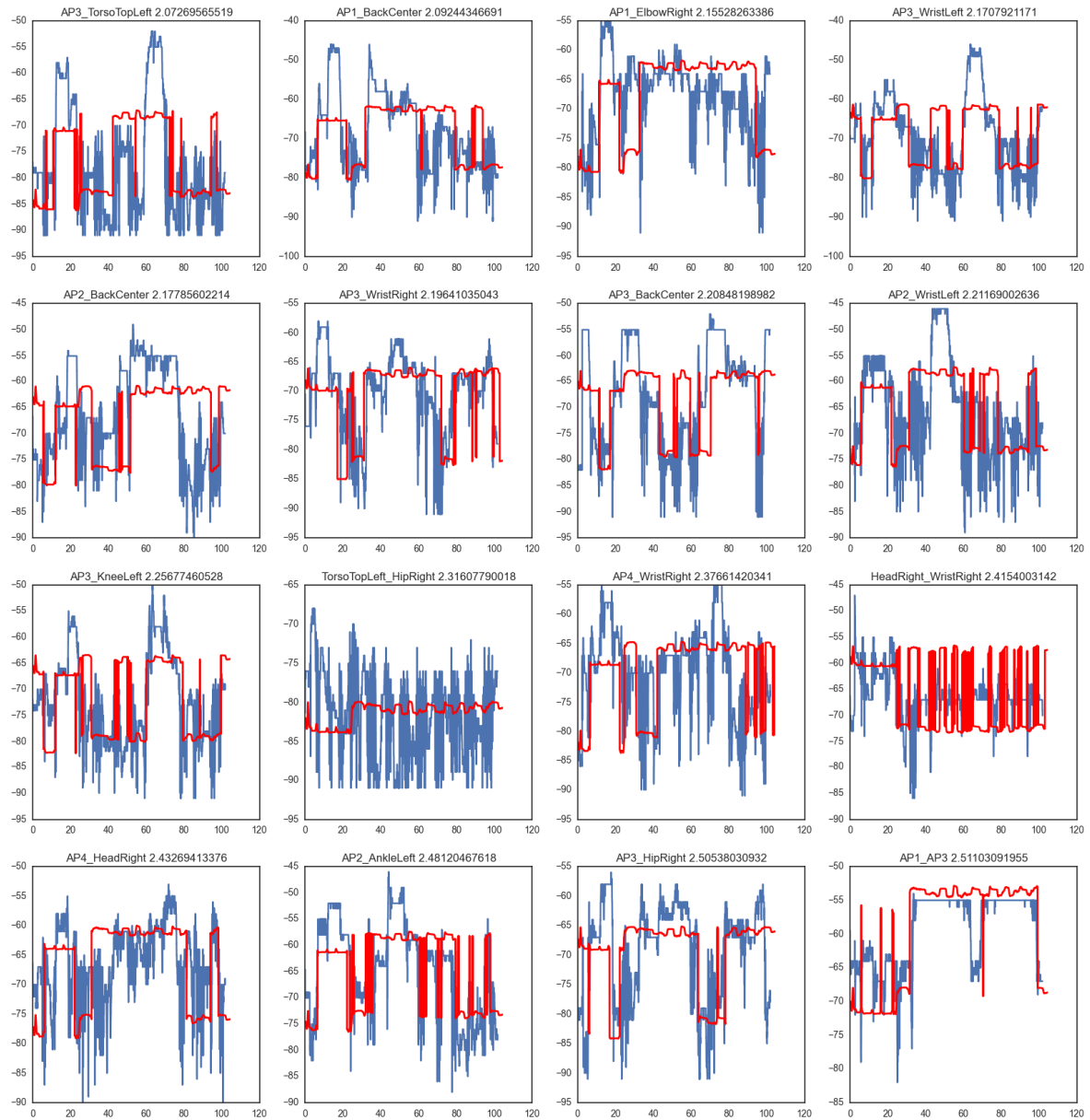


Figure 4.2: Comparison of HKB RSSI (blue) vs centered distance shadowing indicator from MoCap (red) time series, 16 sorted less correlated links (Scenario Sc21.a, Series 6).

4.2. DEMONSTRATION/MEASUREMENT DATABASE ACCESS AND EXPLOITATION

As already mentioned before, the CORMORAN measurement/demonstration campaign is the first known evaluation framework in a jointly heterogeneous, cooperative and mobile WBAN context, gathering:

- 3 different radio technologies;
- Up to 24 radio devices equipping each single body;

- A precise capture of the radio device and body movement using a Vicon motion capture (MoCap) system;
- A perfect knowledge of the capture environment;
- 58 Series with capture or group navigation scenarios;

One major particularity lies in the use of the precise motion capture system simultaneous during radio acquisitions, which allows to get a ground truth position of any involved radio device, thus making the observable radio values open to insightful interpretations (e.g., regarding their link with body mobility).

We introduce hereafter the software environment and tools enabling the exploitation of the collected measurement/demonstration data.

4.2.1 EXPLOITATION IN THE PYLAYERS FRAMEWORK

- *Motivation for Creating a Specific Software Exploitation Tool*

Keeping in mind that one expected outcome of the CORMORAN project is to provide a co-simulation platform coupling realistic physical representations (mobility, antenna and propagation channel) with upper layers (in particular, the MAC layer), a first dedicated software tool has been created to exploit the collected measurement /demonstration data. The latter tool naturally takes place inside the PyLayers simulation framework [PyLayers] (i.e., at the core of the physical simulation engine), as developed in sub-task ST2.4 and successively reported in both D2.5 [CORMORAN_D2.5] and D2.6 [CORMORAN_D2.6].

The creation of this specific software tool has been motivated by the intrinsic complexity of the measurement campaign. First, no existing means was able to directly handle simultaneously the radio and MoCap information out of the collected raw measurements.

In particular, the co-existence of 3 different radio technologies implies 3 different file formats during the collection phase, which have to be interpreted and re-combined together to be exploitable in a jointly heterogeneous and cooperative WBAN context. However, as the motion capture system and the 3 different radio access technologies operate at different sample rates, this led to manipulating 4 different time bases, as illustrated previously with the description of the time-reconciliation procedure. Furthermore no automatic start-synchronization mechanism was available between the different technologies, resulting in non-systematic time shifts between the different bases and traces.

Finally, another aim of the measurement/demonstration campaign was to provide valuable and exploitable information to the project members and more generally, for people in the research community involved in the WBAN field. The goal of this tool is to help and simplify dissemination towards this public as well.

• *Prerequisite Installations*

Before starting using this tool, some preliminary requirements have to be satisfied.

1. The open source platform PyLayers [PyLayers] has to be installed following the installation notes here: <https://github.com/pylayers/pylayers/blob/master/INSTALL.txt>
2. The CORMORAN measurements have to be downloaded from the public repository
3. An environment variable \$CORMORAN has to be set at the root of the CORMORAN measurements directory (help about setup of environment variables can be found in PyLayers' INSTALL.txt).

Once those 3 steps are satisfied, the CORMORAN measurement/demonstration data exploitation tool is ready to be used. In the following, we provided illustrating examples for both the commands and the results to commands (See parts of the text highlighted in cyan below).

• *The CorSer Class*

In the PyLayers environment, the data exploitation takes place as a specific class named CorSer (which stands for Cormoran Series). Once PyLayers has been installed, it is possible to directly access to the class by importing it, as follows:

```
>>> from pylayers.measures.cormoran import *
```

Get information on the Series

Before creating the CorSer object, it is possible to consult the available measurements series using `cor_log()`.

Then for each **series** of a given **day**, it is possible to get:

- The involved subject(s);
- The involved radio technology;
- A short description of the series.

One illustrating example follows:

```
>>> cor_log()
series day      Subject      techno \
0      1  11      Bernard      TCR
1      2  11      Bernard      TCR
2      3  11      Bernard      TCR
3      4  11      Bernard      TCR
4      5  11      Nicolas     HKB+BS
5      6  11      Nicolas     HKB+BS
6      7  11      Nicolas     HKB+BS
7      8  11      Nicolas     HKB+BS
8      9  11      Bernard      TCR
```

9	10	11	Bernard	TCR
10	11	11	Bernard	TCR
11	12	11	Bernard	TCR
12	13	11	Nicolas	HKB+BS
13	14	11	Nicolas	HKB+BS
14	15	11	Nicolas	HKB+BS
15	16	11	Nicolas	HKB+BS
16	17	11	Bernard	TCR
17	18	11	Bernard	TCR
18	19	11	Bernard	TCR
19	20	11	Bernard	TCR
20	21	11	Nicolas	HKB+BS
21	22	11	Nicolas	HKB+BS
22	23	11	Nicolas	HKB+BS
23	24	11	Nicolas	HKB+BS
24	25	11	Bernard	TCR
25	26	11	Bernard	TCR
26	27	11	Nicolas	HKB+BS
27	28	11	Nicolas	HKB+BS
28	29	11	Nicolas	HKB+BS
29	30	11	Nicolas	HKB+BS
30	31	11	Nicolas	HKB+BS
31	32	11	Nicolas	TCR+HKB+BS
32	33	11	Nicolas	TCR+HKB+BS
33	34	11	Nicolas	TCR+HKB+BS
34	35	11	Nicolas	TCR+HKB+BS
35	1	12	Nicolas Jihad Eric	TCR
36	2	12	Nicolas Jihad Eric	TCR
37	3	12	Nicolas jihad Eric	TCR
38	4	12	Nicolas Jihad Eric	TCR
39	5	12	Nicolas Jihad Eric	TCR
40	6	12	Nicolas Jihad Eric	TCR
41	7	12	Nicolas Jihad Eric	TCR
42	8	12	Nicolas Jihad Eric	TCR
43	9	12	Nicolas Jihad Eric	TCR+HKB+BS
44	10	12	Nicolas Jihad Eric	TCR+HKB+BS
45	11	12	Nicolas Jihad Eric	TCR+HKB+BS
46	12	12	Nicolas Jihad Eric	TCR+HKB+BS
47	13	12	Nicolas Jihad Eric	TCR+HKB+BS
48	14	12	Nicolas Jihad Eric	TCR+HKB+BS
49	15	12	Nicolas Jihad Eric	TCR+HKB+BS
50	16	12	Nicolas Jihad Eric	TCR+HKB+BS
51	17	12	Nicolas Jihad Eric	HKB+BS
52	18	12	Nicolas Jihad Eric	HKB+BS
53	19	12	Nicolas Jihad Eric	HKB+BS
54	20	12	Nicolas Jihad Eric	HKB+BS
55	21	12	Nicolas Jihad Eric	HKB+BS
56	22	12	Nicolas Jihad Eric	HKB+BS
57	23	12	Nicolas Jihad Eric	HKB+BS

58 24 12 Nicolas Jihad Eric HKB+BS

Short Notes

0 Subject Walk circularly

1 Subject Walk circularly

2 Subject Walk circularly

3 Subject Walk circularly

4 Subject Walk circularly

5 Subject Walk circularly

6 Subject Walk circularly

7 Subject Walk circularly

8 INTERRUPTED Subject Walk circularly ++ speed

9 Subject Walk circularly ++ speed

10 Subject Walk circularly ++ speed

11 Subject Walk circularly ++ speed

12 Subject Walk circularly without Looking BS pho...

13 Subject Walk circularly + Navigation movement

14 Subject Walk slowly without Looking BS phone h...

15 Subject Walk slowly without Looking BS phone h...

16 Static subject pointing corners then yoga post...

17 Static subject pointing corners then yoga post...

18 Static subject pointing corners then yoga post...

19 Static subject pointing corners then yoga post...

20 Static subject pointing corners (withphone) th...

21 Static subject pointing corners (withphone) th...

22 INTERRUPTED Static subject pointing corners (w...

23 Static subject pointing corners (withphone) th...

24 Kung-fu Kata

25 Kung-fu Kata with Lost sensor

26 subject open door, sit, type on Leyboard, take...

27 subject open door, sit, type on Leyboard, take...

28 Crossfade Yoga Posture with phone BS Left hand

29 Crossfade SLOW Yoga Posture with phone BS Lef...

30 Subject Walk circularly

31 3 turns circularly inc. speed sequentially

32 3 turns circularly inc. speed sequentially

33 3 turns circularly inc. Speed + muscle-buildi...

34 3 turns circularly inc. Speed + muscle-buildi...

35 DATA ISSUE 3 FireMen Nav

36 3 FireMen Nav (possible mocap issue)

37 3 FireMen Nav (possible mocap issue)

38 INTERRUPTED 3 FireMen Nav

39 subjects Random walk + new interfering subject...

40 subjects Random walk + new interfering subject...

41 subjects slow Random walk + interfering subjec...

42 subjects slow Random walk + interfering subjec...

43 SubjectSlow motion: Indoor Nav then Firemen t...

44 SubjectSlow motion: Indoor Nav then Firemen t...

45 Subjectnormal speed: Indoor Nav then Firemen ...


```
46 Subjectnormal speed: Indoor Nav then Firemen ...
47 subjects Random walk + new interfering subject...
48 subjects Random walk + new interfering subject...
49 subjects Random walk + new interfering subject...
50 subjects Random walk + new interfering subject...
51 NO HKB Subjectnormal speed: Indoor Nav then F...
52 NO HKB Subjectnormal speed: Indoor Nav then F...
53 NO HKB Subjectnormal speed: Indoor Nav then F...
54 NO HKB Subjectnormal speed: Indoor Nav then F...
55 subjects Random walk + new interfering subject...
56 subjects Random walk + new interfering subject...
57 subjects Random walk + new interfering subject...
58 subjects Random walk + new interfering subject...
```

Loading Series

As an example, series 6 from day 11/06/2014 can be loaded using the following command:

```
>>> S=CorSer(series=6,day=11)
```

```
Load infrastructure node position: **** Processor coding : Intel-PC
```

```
Load Nicolas body: **** Processor coding : Intel-PC
```

```
BS data frame index: Align on mocap OK... WARNING time-offset NOT applied
No BS offset not yet set => use self.offset_setter
```

```
HKB data frame index: Align on mocap OK... time-offset applied OK
```

```
Create distance Dataframe... OK
```

Once loaded, further information about the series (date, type...) can be obtained just by calling the object itself, as follows:

```
>>> S
Filename: Sc20_S6_R2_HKBS
Day : 11/06/2014
Series : 6
Scenario : 20
Run : 2
Type : HKBS
Original Video Id : Single
Subject(s) : Nicolas
```

```
Body available: True
```

```
BeSPoon : Sc20_S6_R2_HKBS.csv
HIKOB : Sc2_0_S6_r2_HKB_Single.mat
```

Radio DataFrames

Data frames are *Pandas* objects, which can be interpreted as tables;

- Each line corresponds to a given timestamp;
- Each column corresponds to a given link between 2 radio devices.

Depending on the available RAT involved in the series, different data frames are available:

- HiKoB (HKB) data : *S.hkb*;
- BeSpoon data : *S.bespo*;
- TCR data : *S.tcr*.

In the chosen illustrating series, only HiKoB and Bespoon are available. Hereafter is another example accounting for the RSSI values issued at the HKB wireless sensors for the 120 available links and the 5 first available timestamps:

```
>>> S.hkb.head(5)
```

```

      AP1-AP2  AP1-AP3  AP1-AP4  AP1-HeadRight  AP1-TorsoTopRight  \
0.000000      NaN      NaN      NaN           NaN           NaN
0.010001      NaN      NaN      NaN           NaN           NaN
0.020002     -60     -64     -61           -71           -81
0.030003     -60     -64     -61           -71           -81
0.040004     -60     -64     -61           -71           -81
```

```

      AP1-TorsoTopLeft  AP1-BackCenter  AP1-ElbowRight  AP1-ElbowLeft
\
0.000000              NaN              NaN              NaN              NaN
0.010001              NaN              NaN              NaN              NaN
0.020002             -73             -78             -79             -84
0.030003             -73             -78             -79             -84
0.040004             -73             -78             -79             -84
```

```

      AP1-HipRight  ...  WristRight-WristLeft  \
0.000000          NaN  ...              NaN
0.010001          NaN  ...              NaN
0.020002          -73  ...              -64
0.030003          -73  ...              -64
0.040004          -73  ...              -64
```

```

      WristRight-KneeLeft  WristRight-AnkleLeft  WristRight-AnkleRight
\
0.000000              NaN              NaN              NaN
0.010001              NaN              NaN              NaN
0.020002             -88             -64             -55
0.030003             -88             -64             -55
0.040004             -88             -64             -55
```

```

      WristLeft-KneeLeft  WristLeft-AnkleLeft  WristLeft-AnkleRight  \
```

0.000000	NaN	NaN	NaN
0.010001	NaN	NaN	NaN
0.020002	-63	-61	-77
0.030003	-63	-61	-77
0.040004	-63	-61	-77

	<i>KneeLeft-AnkleLeft</i>	<i>KneeLeft-AnkleRight</i>	<i>AnkleLeft-AnkleRight</i>
0.000000	NaN	NaN	NaN
0.010001	NaN	NaN	NaN
0.020002	-60	-84	-79
0.030003	-60	-84	-79
0.040004	-60	-84	-79

[5 rows x 120 columns]

Non Radio DataFrames

Extra data frames are also available to access to non-radio information:

- *S.devdf*: the device dataframe, which gives mechanical information: position (x,y,z), velocity (v,vx,vy,vz) and acceleration (a,ax,ay,az) of the devices at any timestamp;
- *S.distdf*: the distance data frame, which gives ground-truth inter-node distances over the different radio links.

As an illustration, the 5 last data values of the device data frame are shown below:

```
>>> S.devdf.tail(5)
```

	id	subject	x	y	z	v	vx	vy	vz	a	ax	ay	az
104.2	HKB:14	Nicolas	0.158588	-1.574102	0.526740	0.012375	-0.005046	0.010521	0.004119	2.241849	1.972888	0.738384	0.767065
104.2	HKB:1		0.018552	-2.749937	0.979166	0.000000	0.000000	0.000000	0.000000	0.000000	0.000000	0.000000	0.000000
104.2	HKB:16	Nicolas	-0.229677	-1.445404	0.175125	0.010563	-0.007414	-0.006640	-0.003540	0.547761	0.122199	-0.250196	-0.471711
104.2	HKB:10	Nicolas	0.262695	-1.433168	1.143153	0.057829	-0.048329	-0.030039	-0.010302	0.924303	-0.697193	0.368582	-0.482085
104.2	HKB:3		0.021135	3.375590	1.003871	0.000000	0.000000	0.000000	0.000000	0.000000	0.000000	0.000000	0.000000

As an illustration, the 5 last data values of the distance data frame are shown below:

```
>>> S.distdf.tail(5)
```

	HKB:1-HKB:2	HKB:1-HKB:3	HKB:1-HKB:4	HKB:1-HKB:5	HKB:1-HKB:6
104.159996	6.102589	6.125578	6.135849	1.308815	1.163639
104.169997	6.102589	6.125578	6.135849	1.309074	1.163713
104.179998	6.102589	6.125578	6.135849	1.309470	1.163938
104.189999	6.102589	6.125578	6.135849	1.309873	1.164064

104.200000	6.102589	6.125578	6.135849	1.310357	1.164289
------------	----------	----------	----------	----------	----------

	<i>HKB:1-HKB:7</i>	<i>HKB:1-HKB:8</i>	<i>HKB:1-HKB:9</i>	<i>HKB:1-HKB:10</i>	<i>HKB:1-</i>
<i>HKB:11 \</i>					
104.159996	1.131707	1.387571	1.322510	1.350930	
1.223406					
104.169997	1.131587	1.387549	1.322884	1.350486	
1.223658					
104.179998	1.131414	1.387530	1.323230	1.350018	
1.223874					
104.189999	1.131319	1.387509	1.323601	1.349608	
1.224129					
104.200000	1.131228	1.387509	1.323915	1.349214	
1.224341					

		<i>HKB:12-HKB:15</i>	<i>HKB:12-HKB:16</i>	<i>HKB:13-HKB:14</i>	<i>\</i>
104.159996	...	1.071233	0.990922	0.411064	
104.169997	...	1.071489	0.990873	0.410944	
104.179998	...	1.071624	0.990832	0.410933	
104.189999	...	1.071955	0.990734	0.410871	
104.200000	...	1.072294	0.990736	0.410651	

	<i>HKB:13-HKB:15</i>	<i>HKB:13-HKB:16</i>	<i>HKB:14-HKB:15</i>	<i>HKB:14-HKB:16</i>	<i>\</i>
104.159996	0.753501	0.910143	0.364396	0.539795	
104.169997	0.753502	0.909901	0.364396	0.539682	
104.179998	0.753522	0.909759	0.364316	0.539533	
104.189999	0.753529	0.909520	0.364281	0.539368	
104.200000	0.753482	0.909291	0.364271	0.539394	

	<i>HKB:15-HKB:16</i>	<i>BS:0-BS:74</i>	<i>BS:0-BS:157</i>
104.159996	0.445009	1.046829	0.119864
104.169997	0.445027	1.046903	0.119868
104.179998	0.445038	1.046936	0.119734
104.189999	0.445063	1.047000	0.119982
104.200000	0.445110	1.046967	0.119830

[5 rows x 122 columns]

Involved devices (S.dev)

The *S.dev* command allows to obtain the complete list of devices involved in the series, as well as:

- The Name of the device used in the radio dataframe;
- The Real device Id used during the measurement campaign;
- The corresponding device Id used on the body wear description;
- The related carrying Subject/body.

Note that the infrastructure access nodes obviously do not have any related carrying Subject/body.

```
>>> S.dev
```

Name in Dataframe	Real Id	Body Id	Subject
AP4	4	HKB:4	
AP1	1	HKB:1	
AP2	2	HKB:2	
AP3	3	HKB:3	
AnkleRight	16	HKB:16	Nicolas
KneeLeft	14	HKB:14	Nicolas
AnkleLeft	15	HKB:15	Nicolas
WristRight	12	HKB:12	Nicolas
WristLeft	13	HKB:13	Nicolas
ElbowLeft	10	HKB:10	Nicolas
HipRight	11	HKB:11	Nicolas
HeadRight	5	HKB:5	Nicolas
TorsoTopRight	6	HKB:6	Nicolas
TorsoTopLeft	7	HKB:7	Nicolas
BackCenter	8	HKB:8	Nicolas
ElbowRight	9	HKB:9	Nicolas
WristRight	157	BS:157	Nicolas
AnkleRight	74	BS:74	Nicolas
HandRight	0	BS:0	Nicolas

Accessing the data

Some methods are also provided in order to extract values from both radio and non-radio dataframes.

Get device position (S.getdevp)

The value of the device position at a specific time (or range or time) can be obtained by specifying:

- The device (Name in dataframe OR real id OR body id);
- The radio techno (Precising the techno is optional except when an ambiguity occurs, therefore an error is raised);
- The given time in second or a [start time, stop time]. If no time is given, the positions for all time stamps are provided.

Hence, as an example, it is possible to get the positions of the HKB radio node 11 (Hip Right), between 5.0 seconds and 5.2 seconds as follows:

```
>>> Positions = S.getdevp(11,t=[5,5.2])
>>> Positions
```

	x	y	z
5.000480	-0.139566	0.224905	1.016796
5.010481	-0.139553	0.224845	1.016826
5.020482	-0.139545	0.224825	1.016818
5.030483	-0.139564	0.224730	1.016849
5.040484	-0.139609	0.224642	1.016859
5.050485	-0.139580	0.224613	1.016898
5.060486	-0.139554	0.224586	1.016920
5.070487	-0.139604	0.224492	1.016937
5.080488	-0.139545	0.224452	1.016989
5.090489	-0.139521	0.224391	1.016992
5.100489	-0.139386	0.224397	1.016997
5.110490	-0.139296	0.224315	1.017041
5.120491	-0.139164	0.224189	1.017098
5.130492	-0.138988	0.224128	1.017131
5.140493	-0.138810	0.224048	1.017142
5.150494	-0.138605	0.223969	1.017148
5.160495	-0.138406	0.223877	1.017164
5.170496	-0.138043	0.223803	1.017230
5.180497	-0.137791	0.223654	1.017305
5.190498	-0.137388	0.223580	1.017321

Get link value (S.getlink)

The values of a link *a* and *b* at a specific time (or range of time) can be obtained by specifying:

- The device *a* (Name in dataframe OR real id OR body id);
- The device *b* (Name in dataframe OR real id OR body id);
- The radio *technoa* and *technob* (Precising the techno is optional except when an ambiguity occurs, therefore an error is raised);
- A given time in second or a [start time,stop time]. If no time is given, the positions for all time stamps are provided;

For instance, it is possible to get the HKB values between radio node 11 (Hip Right) and node 16 (Ankle Right), between 5 seconds and 5.2 seconds with:

```
>>> Values = S.getLink(11,16,t=[5,5.2])
>>> Values
```

5.000500	-67
5.010501	-67
5.020502	-67
5.030503	-67
...	

```
Name: HipRight-AnkleRight, dtype: float64
```


Get link distance (S.getlinkd)

The ground truth distance separating a device *a* and a device *b* at a specific time (or range or time) can be obtained by specifying:

- The device *a* (Name in dataframe OR real id OR body id);
- The device *b* (Name in dataframe OR real id OR body id);
- The radio *technoa* and *technob* (Precising the techno is optional except when an ambiguity occurs, therefore error is raised);
- A given time in second or a [start time,stop time]. If no time is given, the positions for all time stamps are provided.

Hence, as an example, it is possible to get the HKB values between radio node 11 (Hip Right) and node 16 (Ankle Right), between 5 seconds and 5.2 seconds as follows:

```
>>> Distances = S.getlinkd(11,16,t=[5,5.2])
>>> Distances
5.000480    0.845013
5.010481    0.845034
5.020482    0.845045
5.030483    0.845068
5.040484    0.845090
5.050485    0.845180
...*
```

```
Name: HKB:11-HKB:16, dtype: float64
```

Visualizing the Data

Native Pandas Visualization

Because radio data in CorSer are stored into Pandas objects, convenient visualization methods are already available. Most of them can be found here: <http://pandas.pydata.org/pandas-docs/stable/visualization.html>.

As an example (resulting into Figure 4.3), it is possible to display the previous obtained values and distance as follows:

```
>>> # Plotting
... ax=Values.plot() #plot values
>>> l=Distances.plot(secondary_y=True,ax=ax) # plot distances on the right
side
>>>
>>> ##Labelling
... ax.legend() # add Legend box
>>> ax.set_ylabel( 'RSS Values (dBm) ') #set Left ylabel
>>> ax.right_ax.set_ylabel( 'Distances (m) ') #set right ylabel
>>> ax.set_xlabel( 'time (s) ') # set xlabel
>>> ax.set_title( 'Link distance as a function of time ')
```

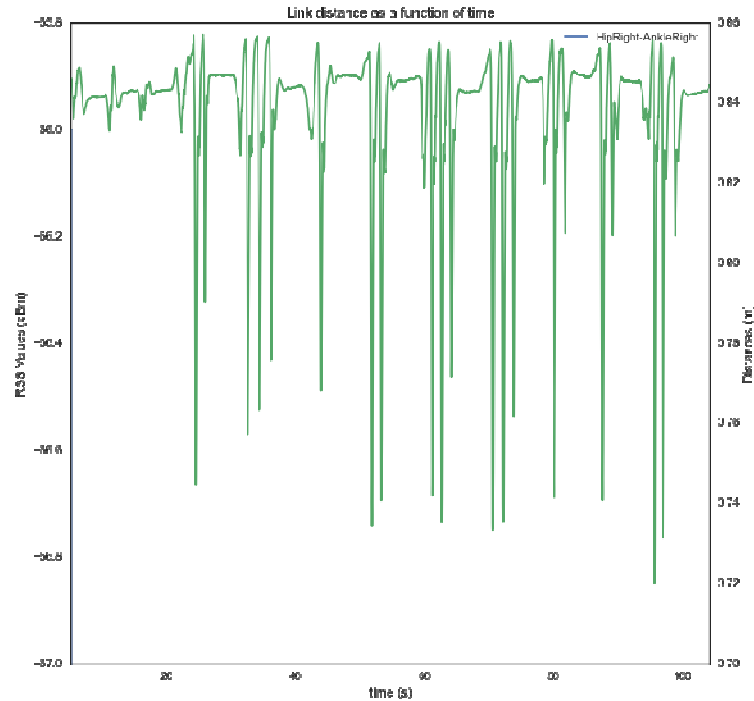


Figure 4.3: Visualization example of a link distance as a function of time.

In addition, CorSer also provides specific plotting methods which includes extra features.

Plot method (S.plot)

The plot function allows to display the radio values of a link. The main parameters are always the same:

- The device *a* (Name in dataframe OR real id OR body id);
- The device *b* (Name in dataframe OR real id OR body id);
- The radio *techno* (Precising the techno is optional except when an ambiguity occurs, therefore an error is raised);
- A given time in second or a [start time,stop time]. If no time is given, the positions for all time stamps are provided.

More option are available, please refer to the docstring (*S.plot?*) for more information

Plot values

Continuing with the same example (resulting into Figure 4.4), it is possible to plot the HKB RSSI values between radio node 11 (Hip Right) and node 16 (Ankle Right), between 5 seconds and 5.2 second, as follows:

```
>>> S.plot(11,16,t=[5,5.2])
```

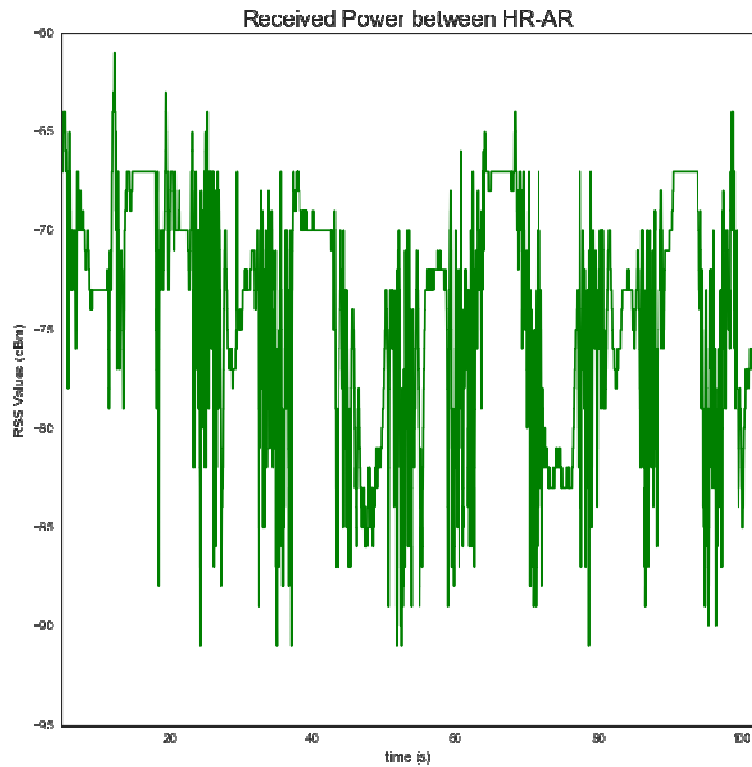


Figure 4.4: Visualization example with RSSI values as a function of time.

Note that it is also possible to get similar results with the following commands:

```
>>>#plotvalue
... f,ax = S.plot(11,16,t=[5,105.2],color = 'b ',title=False)
>>>
>>># create right axis
... ax2=ax.twinx()
>>>
>>> # plot distance
... S.plot(11,16,t=[5,105.2],color = 'g ',title=False,
...       distance=True,
...       fig=f,ax=ax2)
```

Figure 4.5 shows an example superposing both link distance and RSSI values for the same link as previously.

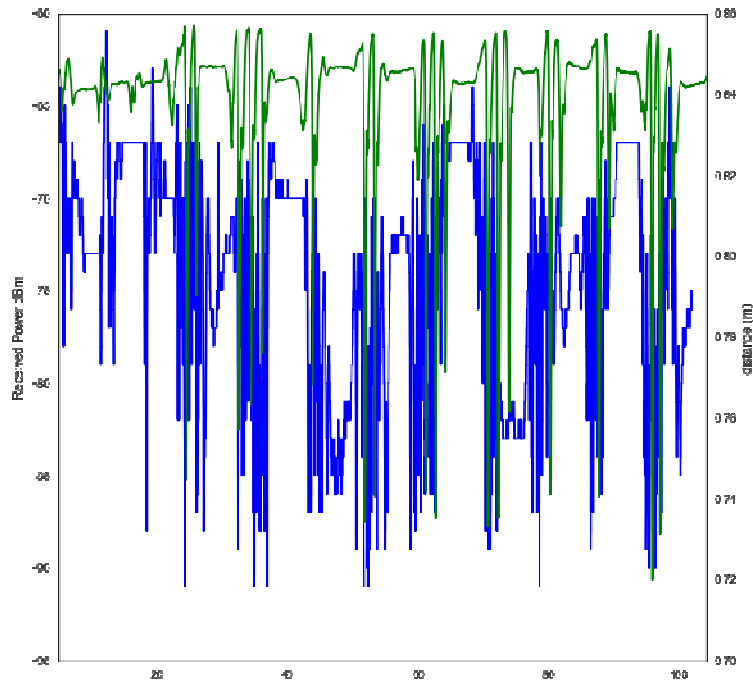


Figure 4.5: Visualization example with superposed link distance and RSSI values as a function of time.

Plot visibility method (S.pltvisi)

In order to go further in the interpretation of collected radio values, it is convenient to have some extra information about the **optical visibility/occultation** of devices involved in a link. In particular, this information allows to determine LoS and NLoS cases, which are crucial for power level and delay analysis. This information can be superposed onto the radio values too. To this end, the plot visibility (*S.pltvisi*) method is used. The **hatched** areas denote **NLOS** cases whereas **clear** areas denote **LOS** cases.

In the provided example below (and on Figure 4.6), the parameters are the same as that used within the *plot* method:

```
>>> f,ax = S.plot(1,16)
>>> S.pltvisi(1,16,fig=f,ax=ax)
```

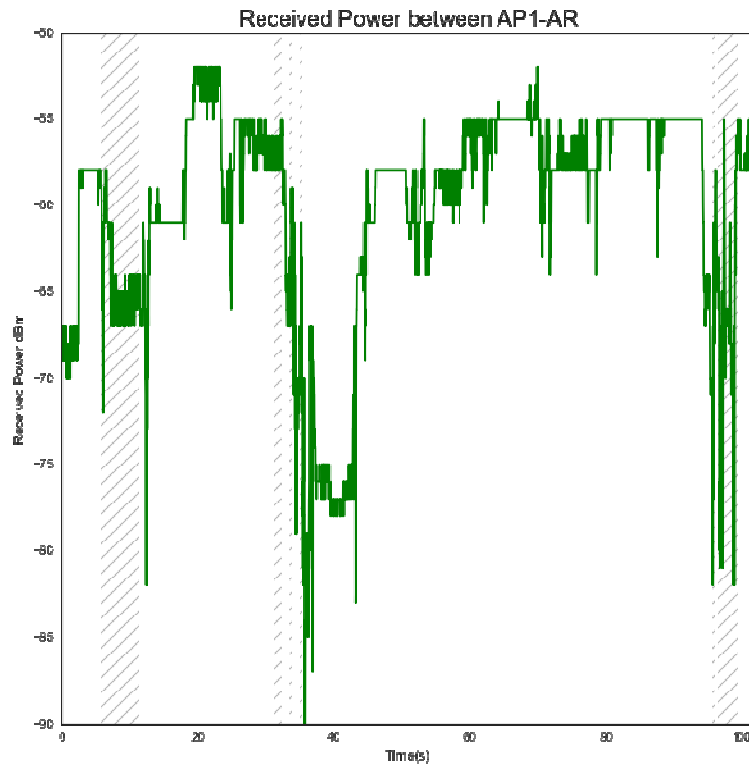


Figure 4.6: Visualization example with superposed RSSI values and LoS/NLoS channel conditions as a function of time.

Plot mobility method (S.pltmob)

It is also possible to determine and indicate whether the carrying subject is static or not, by using the plot mobility method (*S.pltmob*). The succession of Static and Mobile sequences are then denoted by S_x and M_x respectively, where x is an index of the sequence (Figure 4.7).

```
>>> f,ax = S.plot(1,16)
>>> S.pltmob(fig=f,ax=ax)
```

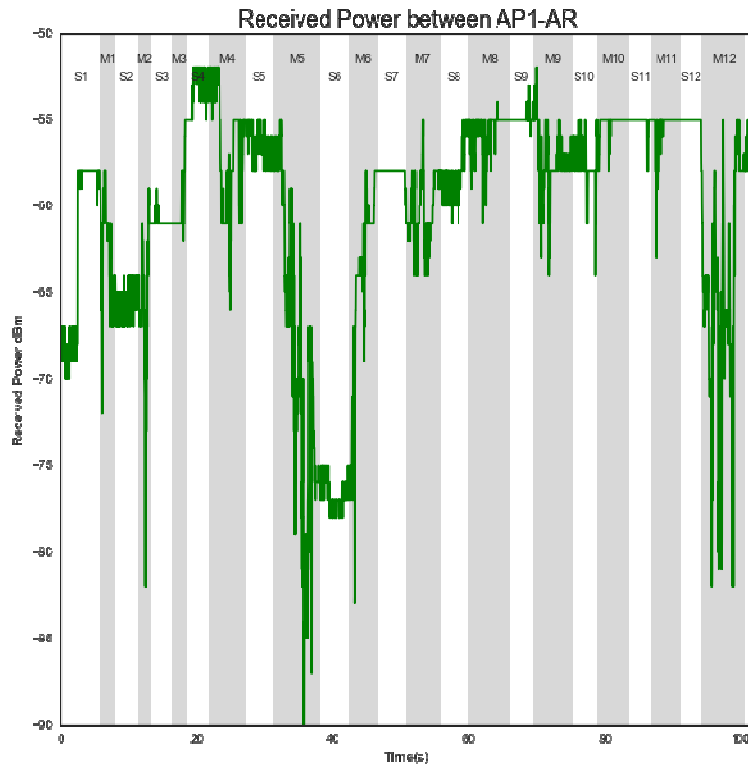


Figure 4.7: Visualization example with superposed RSSI values and Mobile/Static sequences as a function of time.

The 2 methods mentioned above can also be invoked simultaneously, as shown in the following example (Figure 4.8):

```
>>> # plot data in green
... f,ax=S.plthkb(1,13,figsize=(10,5))
>>> # plot optical occultation (hatched lines)
... S.pltvisi(1,13,fig=f,ax=ax)
>>> # plot subject mobility (grey areas)
... S.pltmob(showvel=False,yLim=[-100,-40]),fig=f,ax=ax)
```

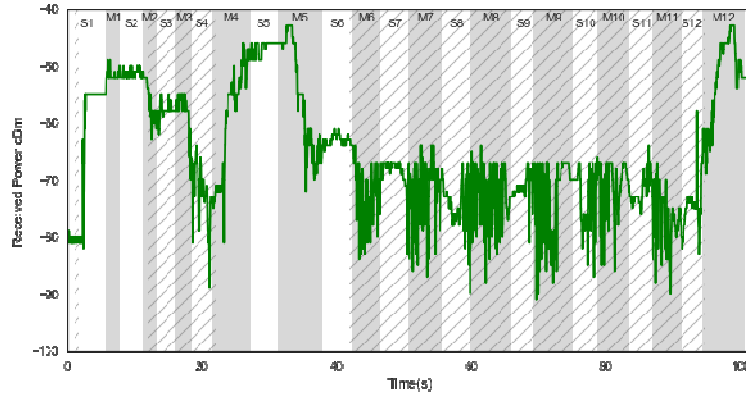



Figure 4.8: Visualization example with superposed RSSI values, LoS/NLoS channel conditions and Mobile/Static sequences as a function of time.

3D plot (*S._show3*)

With the help of the Mayavi Library, the CorSer class enables to display in 3D too, including:

- The building where measurements have taken place;
- The positions of the Vicon Cameras;
- The multi-cylinder representation of the moving subjects involved in the selected series;
- The position/antenna pattern of the devices on the body(ies) and in the infrastructure.

By default, the use of the **S._show3** method displays the complete scene with body(ies) and the associated devices at 4 different timestamp (Figure 4.9).

```
>>> S._show3()
>>>
>>> #the following line is only used to display in the notebook a
screenshot of the mayavi window
```

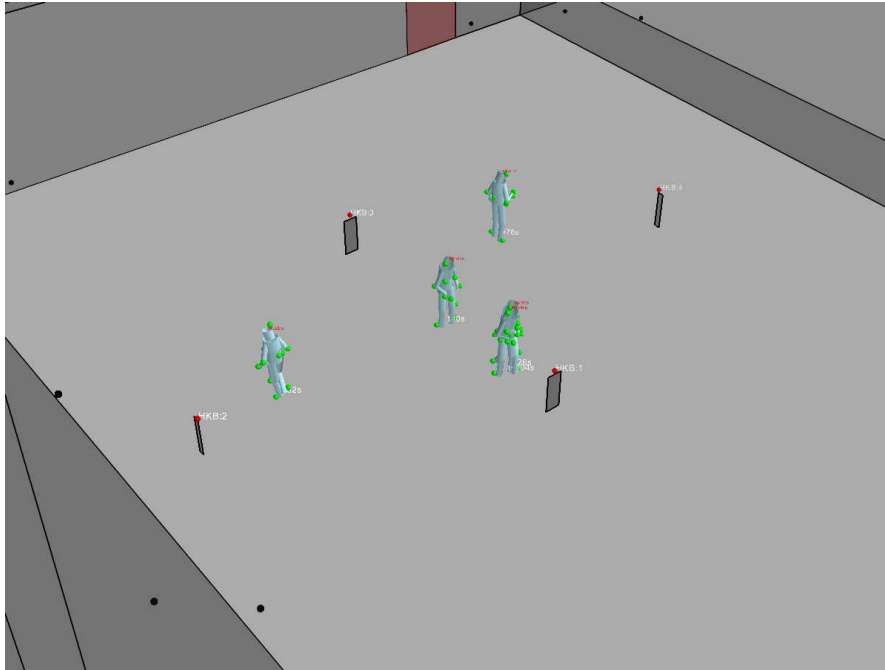


Figure 4.9: Visualization example with one moving equipped subject (grey cylinders) in the entire measurement/demonstration scene at 4 default timestamps, including on-body devices (green spheres) and external anchor nodes (red spheres).

Plot at specified time (bodytime parameter)

In order to display the entire scene at specific timestamps, the parameter *bodytime* can be used. In the example below (Figure 4.10), we consider the body position at $t = 0s$, $t = 30s$ and $t = 90s$.

```
>>> S._show3(bodytime=[0., 30., 90.])
>>>
```

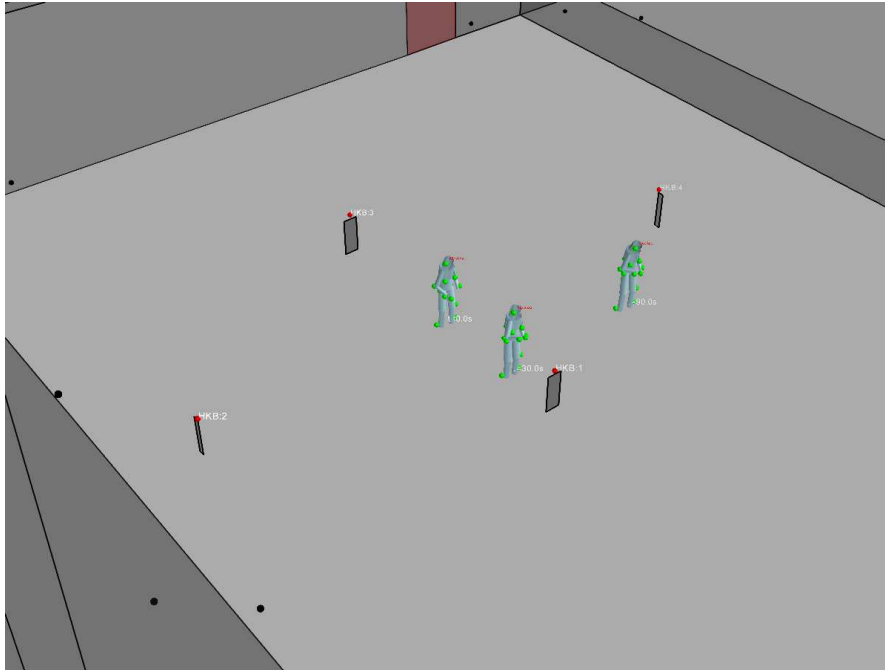


Figure 4.10: Visualization example with one moving equipped subject (grey cylinders) in the entire measurement/demonstration scene at 3 user-specified timestamps, including on-body devices (green spheres) and external anchor nodes (red spheres).

Display a trajectory (trajectory parameter)

So as to materialize also the ground-truth trajectory (Figure 4.11), one can invoke the following command:

```
>>> S._show3(trajectory = True, bodytime=[0., 30., 90.])
>>>
```

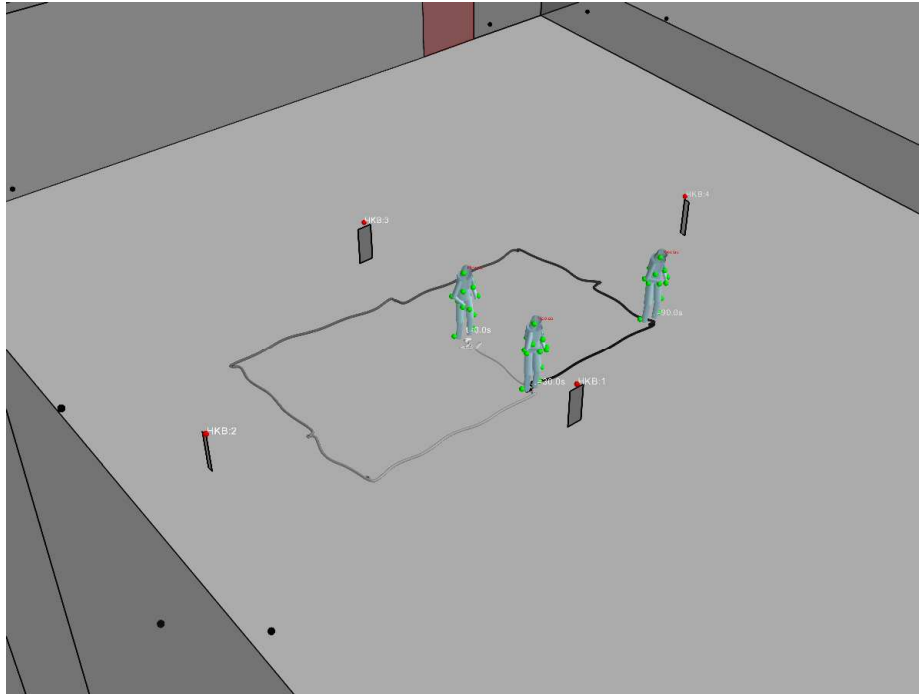


Figure 4.11: Visualization example with one moving equipped subject (grey cylinders) at 3 user-specified timestamps along the full followed trajectory (black path on the floor) in the entire measurement/demonstration scene, including on-body devices (green spheres) and external anchor nodes (red spheres).

*3D plot interactive (*S._show3i*)*

The method **S._show3i()** allows to display the 3D scene with an extra window including a slider acting like a jog shuttle, to choose the timestamp to visualize (Figure 4.12).

```
>>> S._show3i(t=35) #t=35 is an initialization value
```

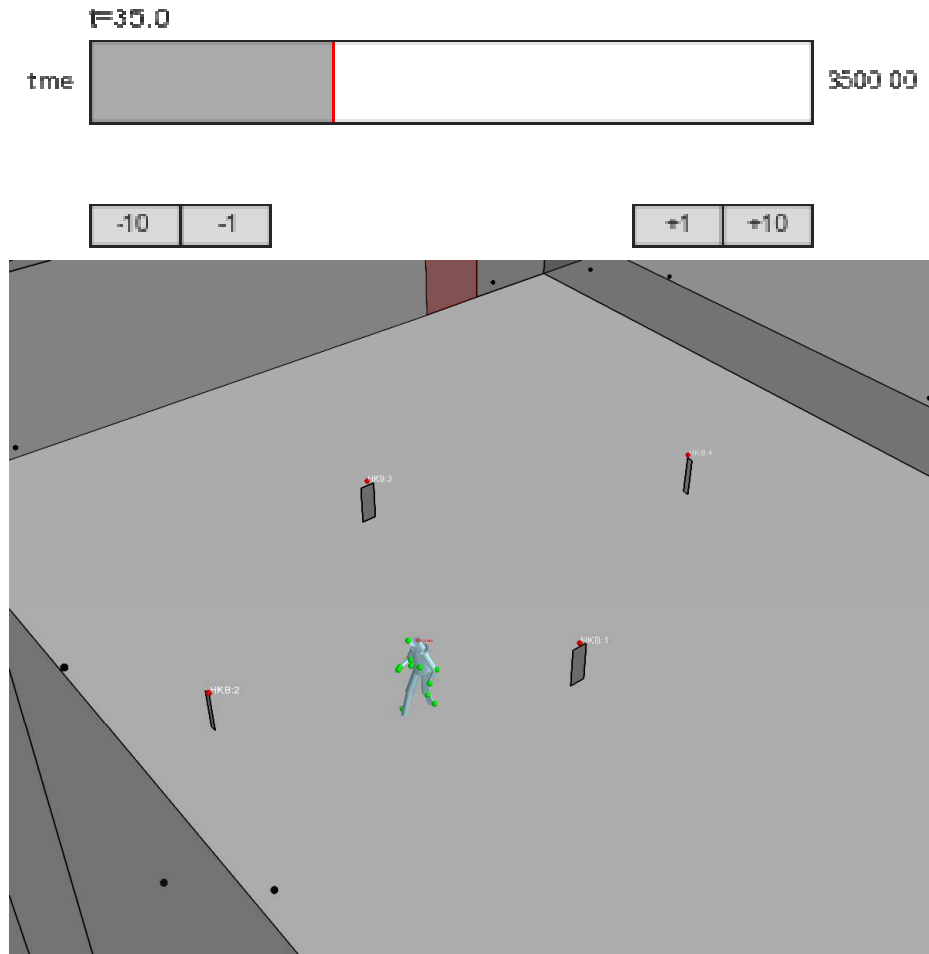


Figure 4.12: Visualization example with one moving equipped subject (grey cylinders) in the entire measurement/demonstration scene at the particular timestamp $t=35s$ according the top slider, including on-body devices (green spheres) and external anchor nodes (red spheres).

Interactive visibility (S.imshowvisibility_i)

The visibility/occultation matrix accounting for link connectivity can be displayed simultaneously to the 3D view. For that purpose, the matrix is computed the first time the visualization is called. As an example, the following code displays the obtained visibility matrix within the associated 3D scene at the initial time $t = 35s$ (Figure 4.13).

```
>>> S.imshowvisibility_i(t=35)
```

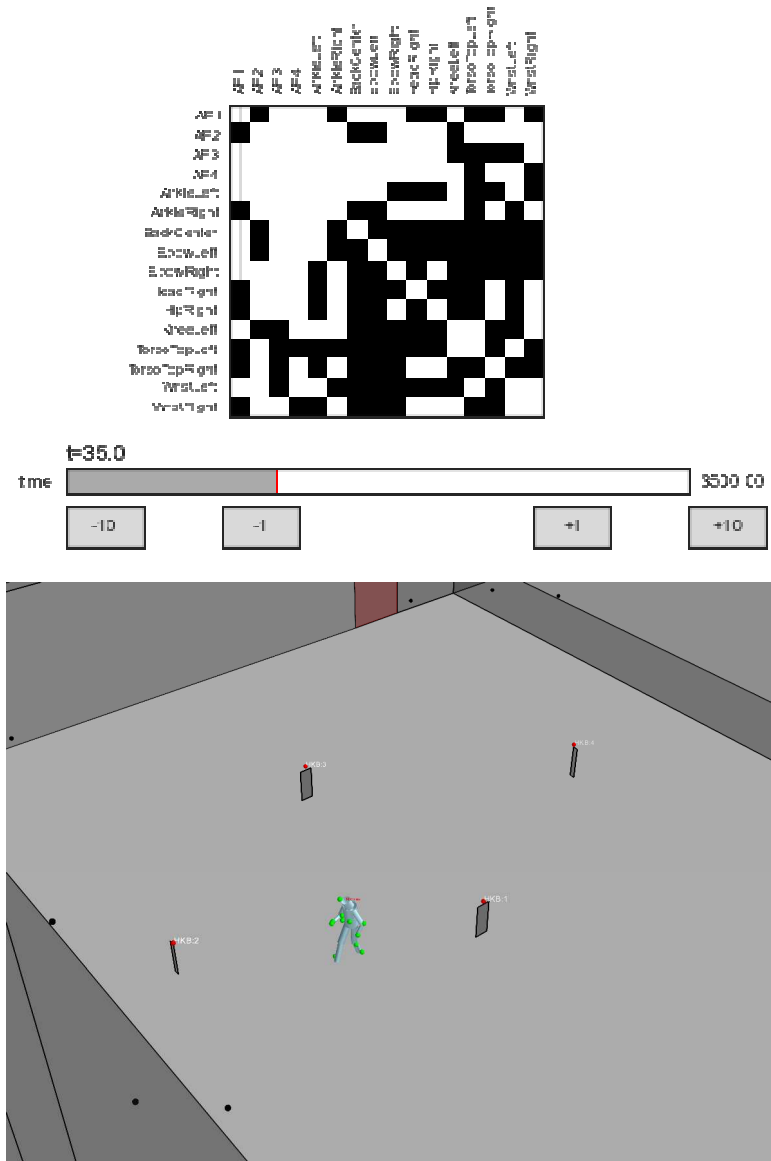


Figure 4.13: Visualization example with one moving equipped subject (grey cylinders) in the entire measurement/demonstration scene at the particular timestamp $t=35s$ according the top slider, including on-body devices (green spheres) and external anchor nodes (red spheres), along with the corresponding on-body/off-body connectivity matrix.

4.2.2 EXPLOITATION AS MATLAB FILES

In this section, we show examples of measurement/demonstration data files, which have been directly converted and repackaged based on the previous software pre-processing tools so as to comply with the Matlab format. This additional step is intended for even easier data usage and exploitation independently of the PyLayers framework (e.g., for direct performance evaluation of algorithms coded in Matlab). Each series of the CORMORAN

measurement/demonstration campaign has thus been put in a single self-contained file. The file naming convention as follows: S{day}_{series}.mat.

Accordingly, for Day 1 (i.e., 11/06/2014) the list of produced files is as follows:

S11_1.mat
S11_2.mat
S11_3.mat
S11_4.mat
S11_5.mat
S11_6.mat
S11_9.mat
S11_10.mat
S11_11.mat
S11_12.mat
S11_13.mat
S11_14.mat
S11_15.mat
S11_16.mat
S11_17.mat
S11_18.mat
S11_19.mat
S11_20.mat
S11_21.mat
S11_22.mat
S11_23.mat
S11_24.mat
S11_25.mat
S11_26.mat
S11_27.mat
S11_28.mat
S11_29.mat
S11_30.mat

For Day 2 (i.e., 12/06/2014), the list comprises:

S12_1.mat
S12_2.mat
S12_3.mat
S12_4.mat
S12_5.mat
S12_6.mat

S12_7.mat
S12_8.mat
S12_9.mat
S12_10.mat
S12_11.mat
S12_12.mat
S12_13.mat
S12_14.mat
S13_15.mat
S12_16.mat
S12_21.mat
S12_22.mat
S12_23.mat
S12_24.mat

Once loaded, the data are described as structured, as follows:

```
node_name = S{day}_{series}.node_name % names of the radio nodes
node_place = S{day}_{series}.node_place % body position of the radio nodes
node_coord = S{day}_{series}.node_coord % coordinates of the radio nodes

tm = S{day}_{series}.tm % time base mocap
```

If the series corresponds to a scenario including shadowing by moving agents:

```
Bernard % centroid of 5 Bernard markers
Claude % centroid of 5 Claude markers
Anis %
Benoit %
Meriem %
```

If the series comprises Hikob data/devices:

```
trh= S{day}_{series}.trh % time base HKB
S{day}_{series}
  HKB.{linkname}.rssi % measured rssi (dBm)
  HKB.{linkname}.dist % link distance
  HKB.{linkname}.sh % link shadowing based on body cylinder
  % approximation
  HKB.{linkname}.dsh % indicator combination of distance and shadowing
```

If the series comprises TCR data/devices:

```
trt = S{day}_{series}.trt % time base TCR

S{day}_{series}
HKB.{linkname}.range % measured rssi (dBm)
HKB.{linkname}.dist % link distance
HKB.{linkname}.sh % link shadowing based on body cylinder
% approximation
```

5. CONCLUSION

This D4.1 deliverable accounts for two localization-oriented measurement/demonstration campaigns based on real integrated radio devices in a cooperative and multi-standard WBAN context.

The ambition of these campaigns was three-fold: i) provide realistic test vectors to evaluate, benchmark and demonstrate in sub-task ST4.3 key algorithms developed in sub-task ST3.x; ii) support the development of a deterministic simulation tool in sub-task ST2.4 (by delivering ground-truth data with the possibility to compare with real radio traces), iii) make available an unprecedented and self-contained measurement database for the interested research community (as one project outcome).

First of all, we have reported a first campaign that was carried out in a confined indoor office room and uniquely based on integrated IR-UWB devices. The objective was mostly to quantitatively validate and characterize on-body single-link ranging errors. Different sets of peer-to-peer RT-ToF measurements have thus been collected and analyzed, taking into account LOS and NLOS conditions over on-body links, and more marginally, over off-body links. The obtained results are at least partly compliant with the on-body models proposed in [Hamie13], where zero-mean random ranging errors have been assumed under LOS conditions, with an additive positive bias under NLOS conditions that strongly depends on the kind of body obstruction (i.e. partial or complete). On-body and off-body ranging results look also consistent under similar NLOS configurations caused by body shadowing. Besides the preliminary observations and findings regarding ranging performance, other mesh scenarios have also been considered for relative on-body positioning and will be further evaluated in sub-task ST4.3.

For the second extensive campaign, which was carried out in an open environment usually devoted to MoCap, three different kinds of radio devices were involved (including IR-UWB and IEEE 802.15.4 devices at 2.4GHz), along with an accurate MoCap system for space/time referencing. Various scenarios have been tested, including single-user and group configurations, with mobility patterns spanning from the moderate walk (or even jogging) to static postures (e.g., Yoga) or slow successive gestures (e.g., Kung Fu). This campaign enables to cover a variety of applicative contexts (e.g., personal navigation, group navigation for firemen/soldiers, mobility learning and detection with quantitative activity feedback for e-Health or e-Sports...). On this occasion, challenging post-synchronization issues between the different collocated systems have been pointed out and treated (at least in part). Examples of post-synchronized traces have also been illustrated. Finally, the software extraction tools (in compliance with both the PyLayers simulation framework and/or Matlab), as well as the related database formats, have been detailed for further data exploitation in the frame of CORMORAN and beyond.

APPENDICES

5.1. APPENDIX 1: MEASUREMENT LOG AND META DATA (2ND CAMPAIGN)

5.1.1 DAY 1: MOTION CAPTURE AND MOBILITY DETECTION SCENARIOS

Série Générale (VC File)	Série HKB	Scenario n° & Files	Descriptif Sommaire	Time Stamp Macro	
1	N/A	Sc2.0 Sc2.0_S1_r1_TCR_Single VC1	Calibration & validation fonctionnelle TCR / Bernard	15h44	Pas de points cardinaux
2	N/A	Sc2.0 Sc2.0_S2_r2_TCR_Single VC2	Calibration & validation fonctionnelle TCR / Bernard	15h47	Points cardinaux
3	N/A	Sc2.0 Sc2.0_S3_r3_TCR_Single VC3	Calibration & validation fonctionnelle TCR / Bernard	15h49	Marche plus à l'intérieur du rectangle
4	N/A	Sc2.0 Sc2.0_S4_r4_TCR_Single VC4	Calibration & validation fonctionnelle TCR / Bernard	15h51	Bars porté à la partie gauche du visage et au nez
5	1	Sc2.0 Sc2.0_S5_r1_HKB_Single Sc2.0_S5_r1_BS_Single VC5	Calibration & validation fonctionnelle HKB + BS / Nicolas	16h06	
6	2	Sc2.0 Sc2.0_S6_r2_HKB_Single Sc2.0_S6_r2_BS_Single VC6	Calibration & validation fonctionnelle HKB + BS / Nicolas	16h12	
7	3	Sc2.0 Sc2.0_S7_r3_HKB_Single Sc2.0_S7_r3_BS_Single VC7	Calibration & validation fonctionnelle HKB + BS / Nicolas	16h15	
8	4	Sc2.0 Sc2.0_S8_r4_HKB_Single Sc2.0_S8_r4_BS_Single VC8	Calibration & validation fonctionnelle HKB + BS / Nicolas	16h17	
9	N/A	Sc2.1a Sc2.1a_S9_r1_TCR_Single VC9	LSIMC Walk 1-RAT (TCR) / Bernard	16h27	Avorté
10	N/A	Sc2.1a Sc2.1a_S10_r2_TCR_Single VC10	LSIMC Walk 1-RAT (TCR) / Bernard	16h29	
11	N/A	Sc2.1a Sc2.1a_S11_r3_TCR_Single VC11	LSIMC Walk 1-RAT (TCR) / Bernard	16h31	

12	N/A	Sc2.1a Sc2.1a_S12_r4_TCR_Single VC12	LSIMC Walk 1-RAT (TCR) / Bernard	16h33	Accélération dans le virage + posture de bras non naturelle au début
13	5	Sc2.1a Sc2.1a_S13_r1_HKB_Single Sc2.1a_S13_r1_BS_Single VC13	LSIMC Walk 2-RAT (BS+HKB) / Nicolas	16h37	Au départ, balancement naturel avec les bras puis changement avec Spoonphone porté devant le corps (mi-tour)
14	6	Sc2.1a Sc2.1a_S14_r2_HKB_Single Sc2.1a_S14_r2_BS_Single VC14	LSIMC Walk 2-RAT (BS+HKB) / Nicolas	16h39	
15	7	Sc2.1a Sc2.1a_S15_r3_HKB_Single Sc2.1a_S15_r3_BS_Single VC15	LSIMC Walk 2-RAT (BS+HKB) / Nicolas	16h42	Spoonphone non consulté sur la partie lente + Début de consultation sur le 1er demi-tour rapide
16	8	Sc2.1a Sc2.1a_S16_r4_HKB_Single Sc2.1a_S16_r4_BS_Single VC16	LSIMC Walk 2-RAT (BS+HKB) / Nicolas	16h45	
17	N/A	Sc2.1b Sc2.1b_S17_r1_TCR_Single VC17	LSIMC Static Posture (com.+yoga) TCR / Bernard	16h52	
18	N/A	Sc2.1b Sc2.1b_S18_r2_TCR_Single VC18	LSIMC Static Posture (com.+yoga) TCR / Bernard	16h54	
19	N/A	Sc2.1b Sc2.1b_S19_r3_TCR_Single VC19	LSIMC Static Posture (com.+yoga) TCR / Bernard	16h57	
20	N/A	Sc2.1b Sc2.1b_S20_r4_TCR_Single VC20	LSIMC Static Posture (com.+yoga) TCR / Bernard	17h00	
21	9	Sc2.1b Sc2.1b_S21_r1_HKB_Single Sc2.1b_S21_r1_BS_Single VC21	LSIMC Static Posture (com.+yoga) HKB+BS / Nicolas	17h06	
22	10	Sc2.1b Sc2.1b_S22_r2_HKB_Single Sc2.1b_S22_r2_BS_Single VC22	LSIMC Static Posture (com.+yoga) HKB+BS / Nicolas	17h08	

23	11	Sc2.1b Sc2.1b_S23_r3_HKB_Single Sc2.1b_S23_r3_BS_Single VC23	LSIMC Static Posture (com.+yoga) HKB+BS / Nicolas	17h11	Inversion dans le sens du pointage au depart / reprise du mvt à zéro
24	12	Sc2.1b Sc2.1b_S24_r4_HKB_Single Sc2.1b_S24_r4_BS_Single VC24	LSIMC Static Posture (com.+yoga) HKB+BS / Nicolas	17h13	Compteurs non incrémentés sur la vidéo !!! (r4 -> r3)
25	N/A	Sc2.1c Sc2.1c_S25_r1_TCR_sigle VC25	LSIMC Dynamic Kung-Fu TCR / Bernard	17h22	Dos à l'ancre 1
26	N/A	Sc2.1c Sc2.1c_S26_r2_TCR_sigle VC26	LSIMC Dynamic Kung-Fu TCR / Bernard	17h28	Perte de marqueur Vicon au niveau de la pause du « Fox Terrier »
27	13	Sc2.1d Sc2.1d_S27_r1_HKB_Single Sc2.1d_S27_r1_BS_Single VC27	LSIMC Dynamic / Gestes usuels (chaise, etc.) / HKB+BS/Nicolas	17h47	
28	14	Sc2.1d Sc2.1d_S28_r2_HKB_Single Sc2.1d_S28_r2_BS_Single VC28	LSIMC Dynamic / Gestes usuels (chaise, etc.) / HKB+BS/Nicolas	17h48	
29	15	Sc2.1e Sc2.1e_S29_r1_HKB_Single Sc2.1e_S29_r1_BS_Single VC29	LSIMC Dynamic / Yoga enchaîné / HKB+BS/Nicolas	17h51	
30	16	Sc2.1e Sc2.1e_S30_r2_HKB_Single Sc2.1e_S30_r2_BS_Single VC30	LSIMC Dynamic / Yoga enchaîné / HKB+BS/Nicolas	17h53	
31	17	Sc2.0 Sc2.0_S31_r5_HKB_Single Sc2.0_S31_r5_BS_Single VC31	Calibration & validation fonctionnelle HKB + BS / Nicolas	18h00	Série refaite avec de meilleurs résultats qu'au début
32	18	Sc2.1a Sc2.1a_S32_r1_HKB_Joint Sc2.1a_S32_r1_BS_Joint Sc2.1a_S32_r1_TCR_Joint VC32	LSIMC Walk 3-RAT / Nicolas	18h21	
33	19	Sc2.1a Sc2.1a_S33_r2_HKB_Joint Sc2.1a_S33_r2_BS_Joint Sc2.1a_S33_r2_TCR_Joint VC33	LSIMC Walk 3-RAT / Nicolas	18h26	
34	20	Sc2.1a Sc2.1a_S34_r3_HKB_Joint Sc2.1a_S34_r3_BS_Joint Sc2.1a_S34_r3_TCR_Joint	LSIMC Walk 3-RAT / Nicolas	18h32	Accélération jusqu'au trottinement (marche normale,

		VC34			marche rapide, trottinement) puis mouvement de musculation au centre (SpoonPhone le long du corps)
35	21	Sc2.1a Sc2.1a_S35_r4_HKB_Joint Sc2.1a_S35_r4_BS_Joint Sc2.1a_S35_r4_TCR_Joint VC35	LSIMC Walk 3-RAT / Nicolas	18h35	Accélération jusqu'au trottinement (marche normale, marche rapide, trottinement) puis mouvement de musculation au centre (SpoonPhone le long du corps) → Chute du capteur genou TCR en fin de trottinement

5.1.1 DAY 2: NAVIGATION SCENARIOS

Série Générale (VC File)	Série HKB	Scenario n° & Files	Descriptif Sommaire	Time Stamp Macro	Commentaires
1	N/A	Sc2.2a Sc2.2a_S1_r1_TCR_Single VC1	CGN / Marche groupée (nav indoor+pompiers+jogging 2 tours) / TCR / nicolas/jihad/eric	11h17	1 vidéo avortée + Série avortés définitivement au début de la phase pompier (incidents dans la remontée des data dès le 1er tour)
2	N/A	Sc2.2a Sc2.2a_S2_r2_TCR_Single VC2	CGN / Marche groupée (nav indoor+pompiers+jogging) / TCR / nicolas/jihad/eric	11h25	Perte de capteurs optique en fin de 2ème tour
3	N/A	Sc2.2a Sc2.2a_S3_r3_TCR_Single VC3	CGN / Marche groupée (nav indoor+pompiers+jogging) / TCR / nicolas/jihad/eric	11h28	Perte de 2 capteurs optiques en fin de course
4	N/A	Sc2.2a Sc2.2a_S4_r4_TCR_Single VC4	CGN / Marche groupée (nav indoor+pompiers+jogging) / TCR / nicolas/jihad/eric	11h35	(1 vidéo avortée)
5	N/A	Sc2.2b Sc2.2b_S5_r1_TCR_Single	CGN / Marche aléatoire (+ interceptions) / TCR /	11h44	

		VC5	nicolas/jihad/eric		
6	N/A	Sc2.2b Sc2.2b_S6_r2_TCR_Single VC6	CGN / Marche aléatoire (+ interceptions) / TCR / nicolas/jihad/eric	11h47	
7	N/A	Sc2.2b Sc2.2b_S7_r3_TCR_Single VC7	CGN / Marche aléatoire (+ interceptions) / TCR / nicolas/jihad/eric	11h51	
8	N/A	Sc2.2b Sc2.2b_S8_r4_TCR_Single VC8	CGN / Marche aléatoire (+ interceptions) / TCR / nicolas/jihad/eric	11h55	Marche bcp plus lente des porteurs BAN radio
9	1	Sc2.2a Sc2.2a_S9_r1_HKB_Joint Sc2.2a_S9_r1_BS_Joint Sc2.2a_S9_r1_TCR_Joint VC9	CGN / Marche groupée (nav indoor+pompiers+jogging) / 3 RAT / nicolas/jihad/eric	12h34	Très ralenti / Slow motion
10	2	Sc2.2a Sc2.2a_S10_r2_HKB_Joint Sc2.2a_S10_r2_BS_Joint Sc2.2a_S10_r2_TCR_Joint VC10	CGN / Marche groupée (nav indoor+pompiers+jogging) / 3 RAT / nicolas/jihad/eric	12h39	Très ralenti / Slow motion
11	3	Sc2.2a Sc2.2a_S11_r3_HKB_Joint Sc2.2a_S11_r3_BS_Joint Sc2.2a_S11_r3_TCR_Joint VC11	CGN / Marche groupée (nav indoor+pompiers+jogging) / 3 RAT / nicolas/jihad/eric	12h43	Marche normale
	4	Sc2.2a Sc2.2a_S12_r4_HKB_Joint Sc2.2a_S12_r4_BS_Joint Sc2.2a_S12_r4_TCR_Joint VC12	CGN / Marche groupée (nav indoor+pompiers+jogging) / 3 RAT / nicolas/jihad/eric	12h48	
13	5	Sc2.2b Sc2.2b_S13_r1_HKB_Joint Sc2.2b_S13_r1_BS_Joint Sc2.2b_S13_r1_TCR_Joint VC13	CGN / Marche aléatoire (+ interceptions) / 3 RAT / nicolas/jihad/eric	12h53	4 personnes dans le champ (2min)
14	6	Sc2.2b Sc2.2b_S14_r2_HKB_Joint Sc2.2b_S14_r2_BS_Joint Sc2.2b_S14_r2_TCR_Joint VC14	CGN / Marche aléatoire (+ interceptions) / 3 RAT / nicolas/jihad/eric	12h56	5 personnes de nouveau ds le champ
15	7	Sc2.2b Sc2.2b_S15_r3_HKB_Joint Sc2.2b_S15_r3_BS_Joint Sc2.2b_S15_r3_TCR_Joint VC15	CGN / Marche aléatoire (+ interceptions) / 3 RAT / nicolas/jihad/eric	12h59	
16	8	Sc2.2b Sc2.2b_S16_r4_HKB_Joint Sc2.2b_S16_r4_BS_Joint Sc2.2b_S16_r4_TCR_Joint VC16	CGN / Marche aléatoire (+ interceptions) / 3 RAT / nicolas/jihad/eric	13h02	

17	9	Sc2.2a Sc2.2a_S17_r1_HKB_Single Sc2.2a_S17_r1_BS_Single VC17	CGN / Marche groupée (nav indoor+pompiers+jogging) / HKB+BS / nicolas/jihad/eric	13h07	
18	10	Sc2.2a Sc2.2a_S18_r2_HKB_Single Sc2.2a_S18_r2_BS_Single VC18	CGN / Marche groupée (nav indoor+pompiers+jogging) / HKB+BS / nicolas/jihad/eric	13h15	Changement de noeud HKB → Pb avec le noeud 2 (carte SD)
19	11	Sc2.2a Sc2.2a_S19_r3_HKB_Single Sc2.2a_S19_r3_BS_Single VC19	CGN / Marche groupée (nav indoor+pompiers+jogging) / HKB+BS / nicolas/jihad/eric	13h24	Nouveau changement carte SD
20	12	Sc2.2a Sc2.2a_S20_r4_HKB_Single Sc2.2a_S20_r4_BS_Single VC20	CGN / Marche groupée (nav indoor+pompiers+jogging) / HKB+BS / nicolas/jihad/eric	13h27	
21	13	Sc2.2b Sc2.2b_S21_r1_HKB_Single Sc2.2b_S21_r1_BS_Single VC21	CGN / Marche aléatoire (+ interceptions) / HKB+BS / nicolas/jihad/eric	13h30	
22	14	Sc2.2b Sc2.2b_S22_r2_HKB_Single Sc2.2b_S22_r2_BS_Single VC22	CGN / Marche aléatoire (+ interceptions) / HKB+BS / nicolas/jihad/eric	13h33	
23	15	Sc2.2b Sc2.2b_S23_r3_HKB_Single Sc2.2b_S23_r3_BS_Single VC23	CGN / Marche aléatoire (+ interceptions) / HKB+BS / nicolas/jihad/eric	13h36	
24	16	Sc2.2b Sc2.2b_S24_r4_HKB_Single Sc2.2b_S24_r4_BS_Single VC24	CGN / Marche aléatoire (+ interceptions) / HKB+BS / nicolas/jihad/eric	13h39	1 ^{er} obstruction à 30sec (Bernard)

NB: For these trials a spacing of 20cm was maintained between BeSpoon's anchors (clockwise) in comparison with other anchors. A spacing of 10cm was also maintained for the TCR's anchor 4 (anti-clockwise) in comparison with the ground-truth point.

REFERENCES

- [CORMORAN_D1.1] B. Denis, C. Goursaud, et al., “Application Scenarios, System Requirements and Prior Models (Initial Document),” Deliverable D1.1 of the CORMORAN project, June 2012.
- [CORMORAN_D3.1] A. Guizar, et al. “PHY/MAC Cross-layer Design for Enhanced WBAN Communications through Cooperation (Initial Document)”, Deliverable D3.1 of the CORMORAN project, Aug. 2013.
- [CORMORAN_D3.2] B. Denis, et al. “Design of Cooperative Location Algorithms (Initial Document)”, Deliverable D3.2 of the CORMORAN project, Sept. 2013.
- [CORMORAN_D4.2] B. Denis, et al. “Final Demonstrator Test Report”, Deliverable D4.2 of the CORMORAN project, July 2015. (*to appear*)
- [CORMORAN_D2.5] B. Uguen, et al. “First Mobility Enabled Physical Simulator and Coupling with Packet Oriented Simulator”, Deliverable D2.5 of the CORMORAN project, June 2014.
- [CORMORAN_D2.6] B. Uguen, et al. “First Mobility Enabled Physical Simulator and Coupling with Packet Oriented Simulator”, Deliverable D2.5 of the CORMORAN project, Sept. 2015. (*to appear*)
- [Bideau10] B. Bideau, et al. “Using Virtual Reality to Analyze Sports Performance,” in IEEE Computer Graphics and Applications, vol.30, no.2, pp.14-21, March-April 2010.
- [BeSpoon] “BeSpoon SpoonPhone and tags,” <http://spoonphone.com/en/>, 2014.
- [Bucaille07] I. Bucaille, A. Tonnerre, L. Ouvry, and B. Denis, “Mac layer design for uwb ldr systems: Pulsers proposal,” Proc. WPNC’07, pp. 277–283, 2007.
- [CodaMotion] <http://www.codamotion.com>.
- [Cotton14] S.L. Cotton, R. D’Errico and C. Oestges, “A review of radio channel models for body centric communications,” in Radio Science, vol.49, is.6, pp. 371388, June 2014.
- [Denis14] B. Denis, L. Biard, A. Guizar, A. Anoui, C. Goursaud, N. Amiot, M. Mhedhbi, S. Avrillon, E. Plouhinec, B. Uguen, J. Hamie, and C. Chaudet, “Radio-Based Navigation and Posture Detection Experiments in Cooperative Wireless Body Area Networks”, Proc. IEEE ICECS’14, Marseille, Dec. 2014. (*to appear*)
- [Hamie12] J. Hamie, B. Denis, and C. Richard, “Nodes updates censoring and scheduling in constrained decentralized positioning for large-scale motion capture based on wireless body area networks,” Proc. BodyNets’12, pp. 100–105, Sept. 2012.
- [Hamie13] J. Hamie, B. Denis, and C. Richard, “Joint Motion Capture and Navigation in Heterogeneous Body Area Networks with Distance Estimation over Neighborhood Graph,” Proc. WPNC’13, Dresden, March 2013.
- [Hamie13b] J. Hamie, B. Denis, R. D’Errico, and C. Richard, “On-body toa-based ranging error model for motion capture applications within wearable uwb networks,” ACM/Springer Journal of Ambient Intelligence and Humanized Computing, Dec. 2013.
- [Hamie14] J. Hamie, Mickael Maman, and B. Denis, “On-Body Localization Experiments using Real IR-UWB Devices,” Proc. ICUWB’14, Paris, Sept. 2014. (*to appear*)
- [HikoB] “HiKoB FOX sensor,” <http://www.hikob.com/hikob-fox>, 2012.

- [Lachartre09] D. Lachartre, B. Denis, D. Morche, L. Ouvry, M. Pezzin, B. Piaget, J. Prouvee, and P. Vicent, "A 1.1nj/b 802.15.4a-compliant fully integrated uwb transceiver in 0.13 micrometer cmos," Proc. IEEE ISSCS'09, pp. 312–313, 2009.
- [Lauzier13] M. Lauzier, P. Ferrand, A. Fraboulet, H. Parvery, J.-M. Gorce, "Full Mesh Channel Measurements on Body Area Networks under Walking Scenarios," Proc. IEEE EuCAP'13, pp.3508,3512, April 2013.
- [Maman08] M. Maman, B. Denis, M. Pezzin, B. Piaget, and L. Ouvry, "Synergetic mac and higher layers functionalities for uwb ldr-lt wireless networks," Proc. IEEE ICUWB'08, Vol. 3, pp. 101–104, Sept. 2008.
- [Mekonnen10] Z. Mekonnen, E. Slotke, H. Luecken, C. Steiner, and A. Wittneben, "Constrained Maximum Likelihood Positioning for UWB based Human Motion Tracking," Proc. IPIN'10, 2010.
- [Pezzin10] M. Pezzin, D. Lachartre, "A Low Power, Low Data Rate Impulse Radio Ultra Wide Band Transceiver," Proc. FUNEMS'10, June 2010.
- [Rosini12] R. Rosini and R. D'Errico, "Off-body Channel Modelling at 2.45 GHz for Two Different Antennas," Proc. EUCAP'12, pp. 3378-3382, 2012.
- [Shaban10] H. Shaban, M. El-Nasr, and R. Buehrer, "Toward a Highly Accurate Ambulatory System for Clinical Gait Analysis via UWB Radios," in IEEE Trans. Information Technology in Biomedicine, 14(2):284-291, 2010.
- [PyLayers] <http://www.pylayers.org>